Published February 7, 2011

up-regulation of *SOCS3* and *VCAN* (*CSPG2*), two genes responsive to IL-10, was impaired in MoDCs from *STAT3* patients, as demonstrated by comparison with control subjects (Fig. 2 A). Intact signal transduction was observed for TGF-β1, the other critical inhibitory cytokine, in the MoDCs of *STAT3* patients (Fig. S2 E). We evaluated the effect of prior treatment with IL-10 on the phenotypic maturation of MoDCs. IL-10 was added to the culture medium on day 3 of DC differentiation. The prior treatment with IL-10 did not block the differentiation of MoDCs in response to GM-CSF and IL-4 (Fig. S3, A and B) but inhibited the LPS-induced maturation of MoDCs, with inhibition of the up-regulation of co-stimulatory molecules CD80 and CD86 and defective up-regulation of the DC maturation marker CD83 in a control subject. In contrast, the maturation of MoDCs derived from *STAT3* patients showed little sign of inhibition by prior treatment with IL-10 (Fig. S3 C). Up-regulation of CD80, CD83, and CD86 expression by LPS was inhibited by IL-10 pretreatment in control subjects, but the IL-10 pretreatment failed to inhibit the up-regulation of CD80, CD83, and CD86 by LPS in *STAT3* patients (Fig. 2 B). Consistent with this observation, the production of inflammatory cytokines, including TNF, IL-6, and IL-12p40, was suppressed by prior treatment with IL-10 in control subjects. The suppression by IL-10 was severely impaired in the MoDCs from *STAT3* patients (Fig. 2 C). Untreated and IL-10–treated MoDCs were harvested, extensively washed, and co-cultured with third-party allogeneic naive $CD4^+$ T cells from control subjects. LPS-stimulated mature MoDCs induced a significant increase in the uptake of [^{3}H]thymidine by naive $CD4^+$ T cells, with IL-10–treated DCs (IL-10–DCs) from a control subject markedly inhibiting the incorporation of [^{3}H]thymidine. In contrast, the down-regulation was very modest in the IL-10–treated MoDCs from *STAT3* patients. In the absence of MoDCs or naive $CD4^+$ T cells, almost no incorporation of [^{3}H]thymidine was detected (Fig. S4 A). Production of IFN-γ, IL-5, and IL-13 followed a very similar pattern, with prior IL-10 treatment inducing significant down-regulation in control subjects and barely detectable down-regulation in *STAT3* patients (Fig. 2 D). Thus, IL-10 was defective in MoDCs from *STAT3* patients, impairing suppression of (a) the up-regulation of co-stimulatory molecules on MoDCs, (b) the up-regulation of cytokine production by MoDCs, (c) the proliferation of co-cultured naive $CD4^+$ T cells, and (d) cytokine production by co-cultured naive $CD4^+$ T cells.

IL-10 signaling defect in MoDCs leads to the defective generation of tolerogenic DCs and iT_{reg} cells

Control MoDCs up-regulated the expression of inhibitory molecules, including PD-L1, PD-L2, ILT-3, and ILT-4 but not ICOS-L by IL-10 treatment. The up-regulation of these inhibitory molecules was severely impaired in the MoDCs of *STAT3* patients (Fig. 3 A). We then investigated the functional consequences of the defective up-regulation of inhibitory molecules for MoDCs by co-culturing untreated and IL-10–DCs with third-party allogeneic naive $CD4^+$ T cells from control subjects. *FOXP3* messenger RNA (mRNA) levels in $CD4^+$ T cells co-cultured with control IL-10–DCs were approximately four times higher than those for cells co-cultured with untreated control MoDCs. However, up-regulation was severely impaired when naive $CD4^+$ T cells were co-cultured with IL-10–DCs from *STAT3* patients (Fig. 3 B). This observation was confirmed by the cytoplasmic staining of FOXP3 protein and flow cytometric analysis of the $CD4^+$ T cells (Fig. 3 C). This up-regulation of FOXP3 was not likely to be mediated by simple T cell activation because naive $CD4^+$ T cells cultured with control IL-10–DCs proliferated less vigorously compared with those with control DCs and because naive $CD4^+$ T cells cultured with patient DCs proliferated more vigorously compared with those with control DCs in the absence or presence of pretreatment with IL-10 (Fig. S4 B). iT_{reg} cells from control subjects and *STAT3* patients expressed equivalent amount of CD25 on their surface, but the expression levels of CTLA-4 and GITR (glucocorticoid-induced TNFR-related) were up-regulated by the co-culture with control IL-10–DCs, but the up-regulation was impaired by the co-culture with patient IL-10–DCs (Fig. S5).

We further evaluated the consequences of defective FOXP3 up-regulation by investigating iT_{reg} cell activity. Purified $CD4^+CD25^+$ T cells from the co-culture were added to autologous $CD4^+CD25^-$ responder T cells, and the mixture was stimulated with anti-CD3/CD28 mAbs. $CD4^+CD25^+$ T cells cultured with control IL-10–DCs efficiently suppressed the proliferation of CFSE-labeled autologous responder T cells (Fig. 3 D, left, second panel). The suppression of proliferation was severely impaired by $CD4^+CD25^+$ T cells cultured with patient IL-10–DCs (Fig. 3 D, left, third panel). We further evaluated cytokine production by a co-culture of responder T cells and $CD4^+CD25^+$ T cells. The production of IFN-γ, IL-5, and IL-13 was suppressed by co-culture with $CD4^+CD25^+$ cells cultured with control IL-10–DCs (Fig. 3 E). The cytokine production was rather increased by the addition of $CD4^+CD25^+$ T cells cultured with patient IL-10–DCs, which might be caused by decreased iT_{reg} cells and increased activated T cells in this $CD4^+CD25^+$ T cell population from *STAT3* patients. Thus, the IL-10 signaling defect in MoDCs results in the impaired generation of tolerogenic DCs and iT_{reg} cells.

The generation of $FOXP3^+$ iT_{reg} cells is dependent on TGF-β1 (Chen et al., 2003; Coombes et al., 2007; Rubtsov and Rudensky, 2007; Zheng et al., 2007). We therefore investigated the relationship between IL-10–DCs and TGF-β1 in the generation of $FOXP3^+$ iT_{reg} cells. TGF-β1 in the culture medium efficiently up-regulated FOXP3 expression in naive $CD4^+$ T cells in the presence of untreated immature DCs (Fig. 3 F). Control IL-10–DCs up-regulated FOXP3 expression, equivalent to TGF-β1 (Fig. 3 F, fifth dataset vs. third dataset), and a combination of control IL-10–DCs and TGF-β1 (Fig. 3 F, seventh dataset) further up-regulated FOXP3 expression. TGF-β1 effectively up-regulated FOXP3 expression in naive $CD4^+$ T cells when co-cultured with patient DCs, but patient IL-10–DCs were inefficient for the up-regulation

Published February 7, 2011

of FOXP3 expression (Fig. 3 F, sixth dataset). Thus, in addition to TGF-β1, IL-10–DCs play a crucial role in the generation of FOXP3$^+$ iT$_{reg}$ cells. Moreover, these results demonstrated that the defect in FOXP3 up-regulation was not caused by the lack of TGF-β1 in IL-10–DCs from *STAT3* patients because the addition of exogenous TGF-β1 did not rescue this

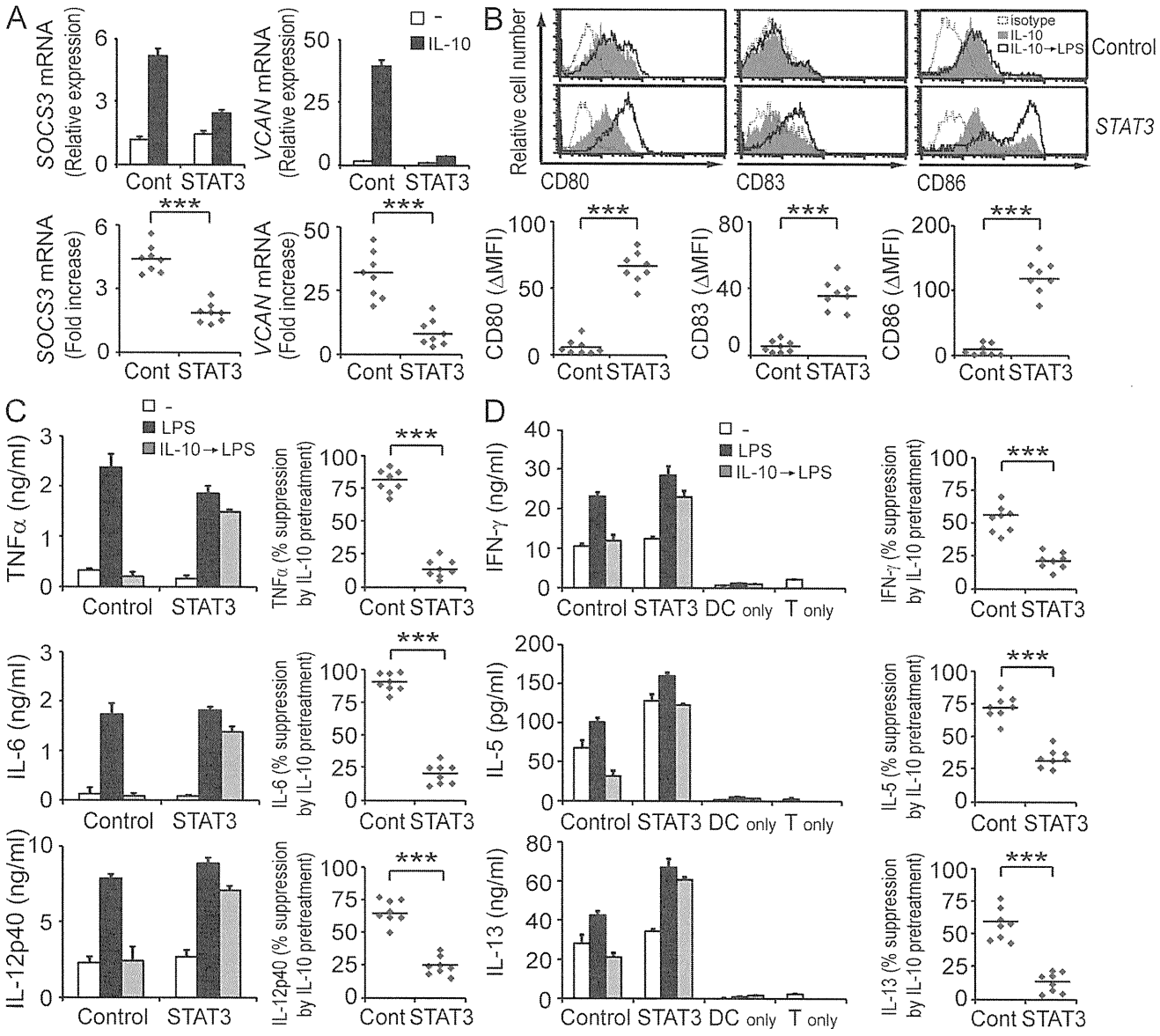

Figure 2. Defective IL-10 signaling in MoDCs from *STAT3* patients. (A) Immature DCs from a control subject and a *STAT3* patient were stimulated with or without IL-10 for 2 h, and the amounts of *SOCS3* and *VCAN* (*CSPG2*) mRNAs were analyzed by Q-PCR. The representative data are shown at the top, normalized to *HPRT* levels, with the level of unstimulated control cells defined as 1.0. Summary data (n = 8 each) showing fold increase are at the bottom. Data are representative of at least two independent experiments performed in triplicate. (B) IL-10–treated MoDCs (IL-10–DCs) were generated from CD14$^+$ monocytes by culturing with GM-CSF and IL-4 in the presence of IL-10 from day 3 of the culture. Representative histograms of CD80, CD83, and CD86 expression of IL-10–DCs (IL-10) and LPS-matured MoDCs after prior treatment with IL-10 (IL-10 → LPS) from a control subject and a *STAT3* patient are at the top. Dashed lines indicate staining with isotype-matched control mAbs. Summary data (n = 8 each) showing delta values of mean fluorescence intensity (ΔMFI), LPS-matured IL-10–DCs minus IL-10–DCs, of CD80, CD83, and CD86 are at the bottom. (C) Representative cytokine levels in the culture supernatants of unstimulated immature MoDCs, LPS-matured MoDCs (LPS), and LPS-matured MoDCs after prior treatment with IL-10 (IL-10 → LPS) from a control subject and a *STAT3* patient are on the left. Summary data (n = 8 each) showing percent suppression are on the right. All samples were evaluated in triplicate. (D) Third-party allogeneic naive CD4$^+$ T cells from control subjects were co-cultured with immature DCs (−), LPS-matured DCs (LPS), or LPS-matured DCs after prior treatment with IL-10 (IL-10 → LPS), and the levels of the cytokines were evaluated by ELISA in triplicate. Representative data are on the left, and summary data of percent suppression by IL-10 pretreatment (n = 8 each) are on the right. Data are representative of at least two independent experiments. (A, C, and D) Graphs show mean ± SD. (A–D) Horizontal bars indicate mean values. ***, $P < 0.001$.

Published February 7, 2011

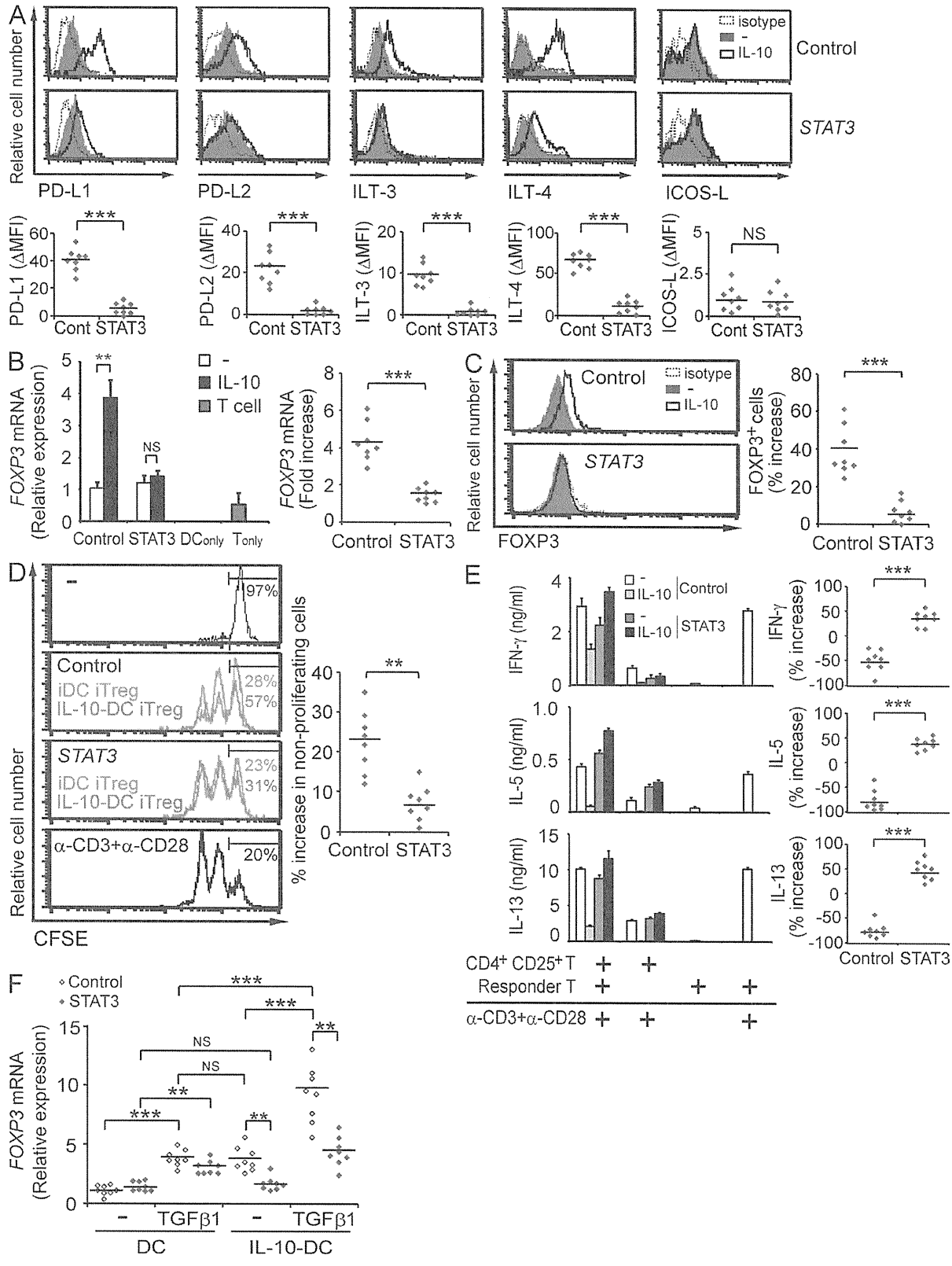

Figure 3. IL-10 signaling defect in MoDCs leads to the defective generation of tolerogenic DCs and iT_{reg} cells. (A) Representative histograms showing the levels of PD-L1, PD-L2, ILT-3, ILT-4, and ICOS-L produced by untreated immature MoDCs (−) and IL-10–DCs (IL-10) from a control subject and a *STAT3* patient are shown at the top. Dashed lines indicate staining with isotype-matched control mAbs. Summary data showing ΔMFI,

Published February 7, 2011

defect to the level of control IL-10–DCs in the presence of TGF-β1 (Fig. 3 F, eighth dataset vs. seventh dataset). To further clarify, we evaluated TGF-β1 and IL-10 production from MoDCs from control subjects and *STAT3* patients (Fig. S6). These results indicate that the production of these inhibitory cytokines from MoDCs is not impaired in *STAT3* patients.

PD-L1, ILT-4, and TGF-β1 in response to IL-10–DCs and STAT3 in DCs play a major role in FOXP3 up-regulation

A recent study in mice demonstrated that PD-L1 plays an important role in inducing FOXP3$^+$ iT$_{reg}$ cells (Keir et al., 2008; Francisco et al., 2009). We investigated whether defective PD-L1 expression in IL-10–DCs from *STAT3* patients played a crucial role in the defective generation of FOXP3$^+$ iT$_{reg}$ cells by adding a peptide neutralizing PD-L1 to the co-culture of IL-10–DCs and naive CD4$^+$ T cells. The addition of this PD-L1 peptide significantly decreased the levels of *FOXP3* mRNA in the naive CD4$^+$ T cells co-cultured with control IL-10–DCs (Fig. 4 A). The addition of the neutralizing peptide had no detectable effect on co-cultures with MoDCs from *STAT3* patients.

We next investigated whether defective ILT-4 expression in IL-10–DCs from *STAT3* patients played an important role in the defective generation of FOXP3$^+$ iT$_{reg}$ cells with a neutralizing mAb to the co-culture of IL-10–DCs and naive CD4$^+$ T cells. The addition of anti–ILT-4 mAb significantly down-regulated the levels of *FOXP3* mRNA in the naive CD4$^+$ T cells co-cultured with control IL-10–DCs compared with a control mAb (Fig. 4 B). The addition of the anti–ILT-4 mAb had no significant effect on the co-culture of the naive CD4$^+$ T cells with patient IL-10–DCs. Thus, in addition to PD-L1, ILT-4 up-regulation in response to IL-10 plays an important role in the generation of FOXP3$^+$ iT$_{reg}$ cells.

We further investigated the contribution of TGF-β1 in the up-regulation of FOXP3 by IL-10–DCs because endogenous TGF-β1 may be supplied by the DCs or from the culture medium. The addition of anti–TGF-β1 mAb significantly down-regulated the levels of FOXP3 mRNA in the naive CD4$^+$ T cells co-cultured with control IL-10–DCs compared with a control mAb (Fig. 4 C). The addition of anti–TGF-β1 mAb had no significant effect on the co-culture of naive CD4$^+$ T cells with patient IL-10–DCs. Thus, TGF-β1 is required for the formation of FOXP3$^+$ iT$_{reg}$ cells in response to control IL-10–DCs.

We also investigated whether DN-STAT3 expression in naive CD4$^+$ T cells plays a significant role in the generation of iT$_{reg}$ cells by evaluating the up-regulation of *FOXP3* mRNA levels in naive CD4$^+$ T cells from *STAT3* patients. The up-regulation of *FOXP3* mRNA levels in response to IL-10–DCs from *STAT3* patients was impaired, but naive CD4$^+$ T cells from control subjects and *STAT3* patients up-regulated *FOXP3* mRNA levels in response to control IL-10–DCs (Fig. 4 D). Thus, DN-STAT3 expression in MoDCs plays a major role in the impairment of *FOXP3* mRNA up-regulation, and DN-STAT3 expression in T cells plays, at most, a minor role in *STAT3* patients.

Primary DCs from *STAT3* patients are defective in IL-10 signaling and up-regulation of PD-L1 and ILT-4

We next investigated the development and function of primary DCs. Two DC subsets were identified in human peripheral blood on the basis of the expression of surface molecules, including CD11c and CD304 (BDCA-4). Lineage marker (Lin) negative HLA-DR$^+$CD11c$^+$CD304$^-$ cells are conventional DCs (cDCs), whereas Lin$^-$HLA-DR$^+$CD11c$^-$CD304$^+$ cells are plasmacytoid DCs (pDCs). The number of PBMCs obtained from the peripheral blood and the percentages of cDCs and pDCs were indistinguishable between control subjects and *STAT3* patients (Fig. 5 A). We next investigated IL-10 signal transduction in primary cDCs and pDCs. The transcriptional up-regulation of *SOCS3* and *VCAN* (*CSPG2*) was impaired in both subsets of primary DCs from *STAT3* patients, as demonstrated by comparison with control subjects (Fig. 5, B and C). We evaluated the effect of prior treatment with IL-10 on the phenotypic maturation of primary cDCs. IL-10 was added to the culture 1 d before LPS treatment, which inhibited the LPS-induced maturation by inhibiting the up-regulation of CD83 and CD86 in control subjects.

IL-10–treated minus untreated, of PD-L1, PD-L2, ILT-3, ILT-4, and ICOS-L (n = 8 each) are at the bottom. (B) Q-PCR analysis of *FOXP3* mRNA levels after the co-culture of third-party allogeneic naive CD4$^+$ T cells from a control subject with untreated immature MoDCs (−) or IL-10–DCs (IL-10) from a control subject and a *STAT3* patient. Cultures in the absence of naive CD4$^+$ T cells (DC only) and MoDCs (T only) were used as negative controls. Representative data are on the left, and summary data (n = 8 each) showing fold increase are on the right. (C) Flow cytometric analysis of cytoplasmic FOXP3 protein levels in naive CD4$^+$ T cells co-cultured with untreated immature MoDCs (−) and IL-10–DCs (IL-10) from a control subject and a *STAT3* patient. Staining with isotype-matched control mAbs is indicated by dashed lines. Representative data are on the left, and summary data (n = 8 each) showing percent increase are on the right. (D) CFSE-labeled CD4$^+$CD25$^-$ responder T cells were cultured alone in the absence (−) or presence of anti-CD3 and anti-CD28 mAbs or with iT$_{reg}$ cells generated by co-culture with control or *STAT3* patient immature DCs (iDCs) or IL-10–DCs. After 5 d, the proliferation of CFSE-labeled responder T cells was assessed by flow cytometry. Representative histograms are on the left, and summary data (n = 8 each) showing the percent increase in nonproliferating cells, numbers in magenta minus numbers in blue, are on the right. (E) Cytokine levels in the supernatants of co-cultures of responder T cells and iT$_{reg}$ cells, as indicated. Representative data are on the left, and summary data (n = 8 each) showing percent increase are on the right. Data are representative of at least two independent experiments. (F) Q-PCR analysis of *FOXP3* mRNA expression after the co-culture of third-party allogeneic naive CD4$^+$ T cells from a control subject with untreated immature MoDCs (−) or IL-10–DCs from a control subject and a *STAT3* patient in the absence or presence of exogenous TGF-β1. We show summary data showing relative *FOXP3* expression (n = 8 each) performed in triplicate. Data are representative of at least two independent experiments. (B and E) Graphs show mean ± SD. (A–F) Horizontal bars indicate mean values. **, $P < 0.01$; ***, $P < 0.001$.

Published February 7, 2011

In contrast, the maturation of primary cDCs derived from *STAT3* patients was almost intact by prior treatment with IL-10 (Fig. 5 D). We did not detect inhibitory effects of IL-10 on CD80 up-regulation in control subjects and *STAT3* patients. Furthermore, control primary cDCs up-regulated the expression of inhibitory molecules, including PD-L1, PD-L2, ILT-3 (unpublished data), and ILT-4 by IL-10 treatment. The up-regulation of these inhibitory molecules was impaired in the primary cDCs of *STAT3* patients (Fig. 5 E). These results demonstrate that IL-10 signaling is defective not only in MoDCs but also in primary DCs, resulting in the defective up-regulation of surface inhibitory molecules in *STAT3* patients.

TYK2-deficient MoDCs are also defective in the generation of tolerogenic DCs and iT_{reg} cells

We studied MoDCs from a patient with *TYK2* deficiency to confirm that the IL-10 signaling defect was responsible for the defective generation of tolerogenic DCs and iT_{reg} cells. The absolute numbers of cDCs and pDCs in PBMCs were similar in the *TYK2*-deficient patient and a control subject, and no significant difference in the differentiation of MoDCs was observed on evaluations of forward and side light scatter, CD1a expression, and the expression of CD80, CD83, and CD86 of DCs before and after LPS-induced maturation (Fig. S7, A–D). No inhibition of the up-regulation of CD80, CD83, and CD86 by prior treatment with IL-10 was detectable in cells from the *TYK2*-deficient patient (Fig. 6 A). The up-regulation of PD-L1, PD-L2, ILT-3, and ILT-4 on MoDCs was also defective in the *TYK2*-deficient patient, as shown by comparisons with control subjects (Fig. 6 B). An increase in *FOXP3* mRNA and protein levels was detectable in co-cultures of allogeneic naive $CD4^+$ T cells with control IL-10-DCs but not in co-cultures with *TYK2*-deficient IL-10–DCs (Fig. 6, C and D). Consistent with these observations, no suppression of naive $CD4^+$ T cell proliferation and cytokine production (including IFN-γ, IL-5, and IL-13) was detected when *TYK2*-deficient IL-10–DCs were used

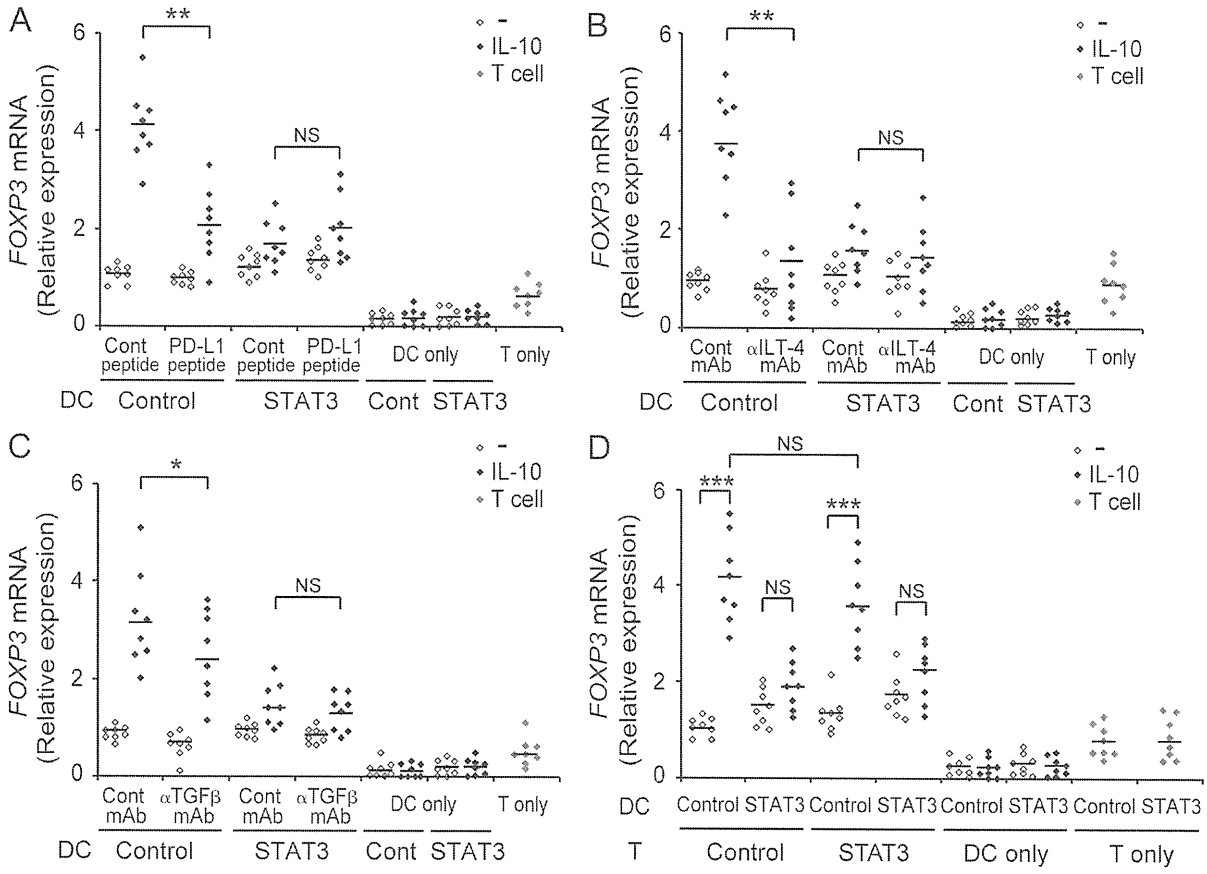

Figure 4. PD-L1, ILT-4, and TGF-β1 in response to IL-10–DCs and *STAT3* in DCs play a major role in FOXP3 up-regulation. (A–C) Q-PCR analysis of *FOXP3* mRNA levels in third-party allogeneic naive $CD4^+$ T cells from control (Cont) subjects co-cultured with untreated immature MoDCs (−) and IL-10–DCs (IL-10) from eight control subjects and eight *STAT3* patients. A neutralizing PD-L1 peptide or a control peptide (A), control or ILT-4–neutralizing mAb (B), or control or TGF-β–neutralizing mAb (C) was added where indicated. (D) Q-PCR analysis of *FOXP3* mRNA levels in third-party allogeneic naive $CD4^+$ T cells from control subjects and *STAT3* patients co-cultured with untreated immature DCs (−) or IL-10–DCs (IL-10) from control subjects and *STAT3* patients. Summary data show relative *FOXP3* mRNA expression ($n = 8$ each) and were performed in triplicate. Data are representative of at least two independent experiments. (A–D) Horizontal bars indicate mean values. *, $P < 0.05$; **, $P < 0.01$; ***, $P < 0.001$.

Published February 7, 2011

(Fig. 6, E and F). MoDCs from the *TYK2*-deficient patient produced an equivalent amount of TGF-β1 and reduced amount of IL-10 compared with a control subject, which might be associated with the fact that the type I IFN signal is impaired in the *TYK2*-deficient patient but not in *STAT3* patients. (Fig. S7, E and F). Thus, the IL-10 signaling defect in HIES patients, *STAT3* patients, and the *TYK2*-deficient patient results in the impaired generation of tolerogenic DCs and iT_{reg} cells.

DISCUSSION

We found that the Th1 and Th2 differentiation of naive $CD4^+$ T cells and the suppressive activity of T_{reg} cells were normal in *STAT3* patients. Recent data have shown that Ig isotype switching in B cells is normal in *STAT3* patients (Avery et al., 2010). Thus, it is not likely that T cell– and B cell–intrinsic mechanisms are responsible for the allergic manifestations in HIES patients. We then investigated DCs, which can regulate the immune response and tolerance. IL-10 signal transduction was defective in the primary DCs and MoDCs of patients, despite the intact TGF-β1 signal transduction in these cells. This defect resulted in impairment of the suppression of cytokine production and T cell proliferation by IL-10–DCs. The generation and suppressive activity of $FOXP3^+$ iT_{reg} cells cultured with IL-10–DCs was impaired in HIES patients. The defective generation of tolerogenic DCs and iT_{reg} cells in response to IL-10 was also observed in the other type of HIES, *TYK2* deficiency. These results suggest that IL-10 signaling in DCs may be crucial for the generation of tolerogenic DCs and iT_{reg} cells to maintain an appropriate Th1–Th2–T_{reg} cell balance in HIES patients.

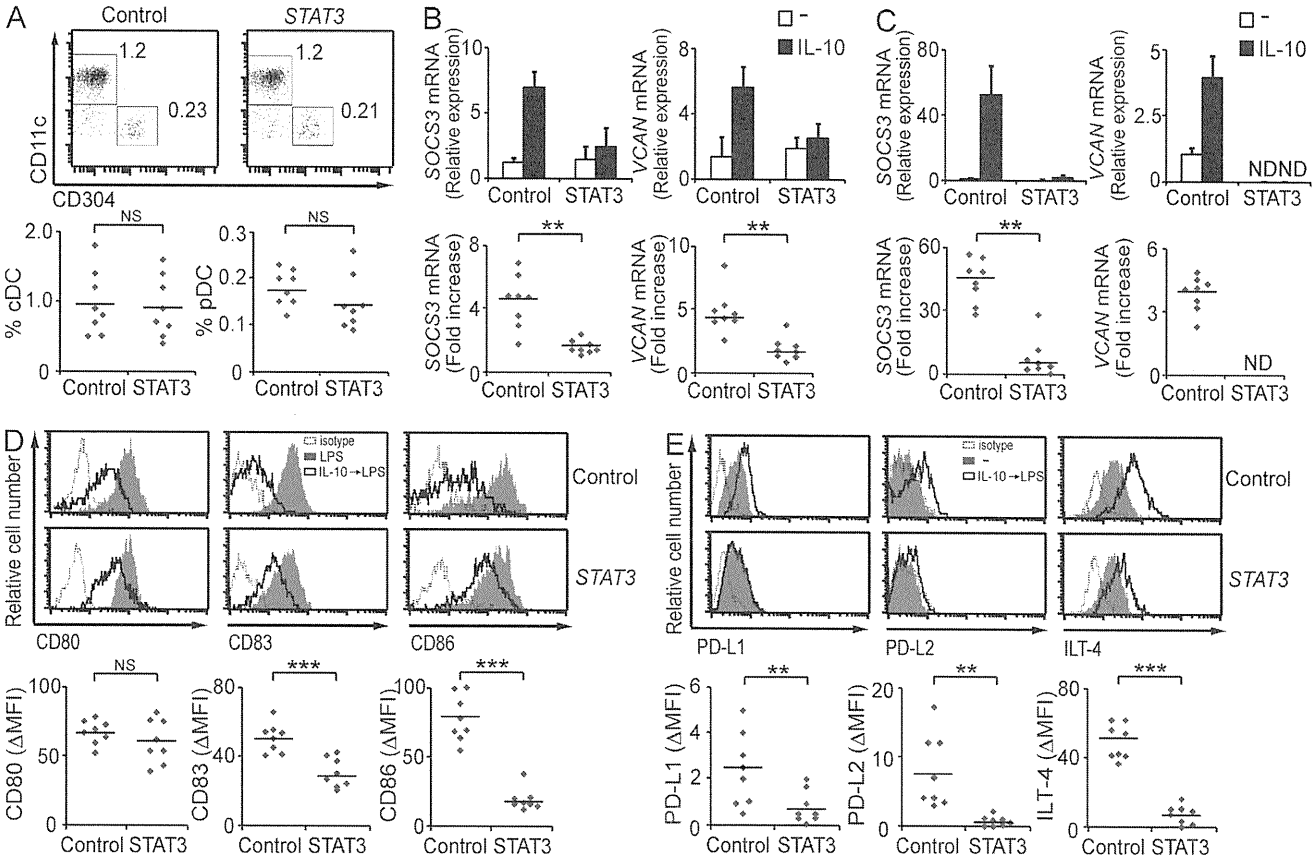

Figure 5. Primary DCs are defective in IL-10 signal and up-regulation of PD-L1 and ILT-4. (A) Dot blots are gated on Lin-negative HLA-DR-positive cells from a control subject and a *STAT3* patient. cDCs are $CD11c^+CD304^-$ (BDCA-4), and pDCs are $CD11c^-CD304^+$. Representative dot plots from a control subject and a *STAT3* patient are shown at the top, and pooled data ($n = 8$ each) showing percentages of cDCs and pDCs are at the bottom. (B and C) Primary cDCs (B) and pDCs (C) from a control subject and a *STAT3* patient were stimulated with IL-10 for 2 h, and the amounts of *SOCS3* and *VCAN* (*CSPG2*) mRNAs were analyzed by Q-PCR. Representative data are shown at the top, normalized to *HPRT* levels, with the level of unstimulated control cells defined as 1.0. Summary data ($n = 8$ each) showing fold increase are at the bottom. Data are representative of at least two independent experiments performed in triplicate. Graphs show mean ± SD. (D) Representative histograms of CD80, CD83, and CD86 expression on control and *STAT3* cDCs stimulated with LPS alone or LPS after IL-10 treatment. Dashed lines indicate staining with isotype-matched control mAbs. Summary data showing ΔMFI, LPS stimulated minus LPS-stimulated IL-10–DCs, ($n = 8$ each) are at the bottom. (E) Representative histograms of PD-L1, PD-L2, and ILT-4 expression of primary cDCs (−) and IL-10–treated (IL-10) primary cDCs from a control subject and a *STAT3* patient are shown at the top. Summary data ($n = 8$ each) showing ΔMFI, IL-10 treated minus untreated, of PD-L1, PD-L2, and ILT-4 are shown at the bottom. Data are representative of at least two independent experiments. (A–E) Horizontal bars indicate mean values. **, $P < 0.01$; ***, $P < 0.001$.

Published February 7, 2011

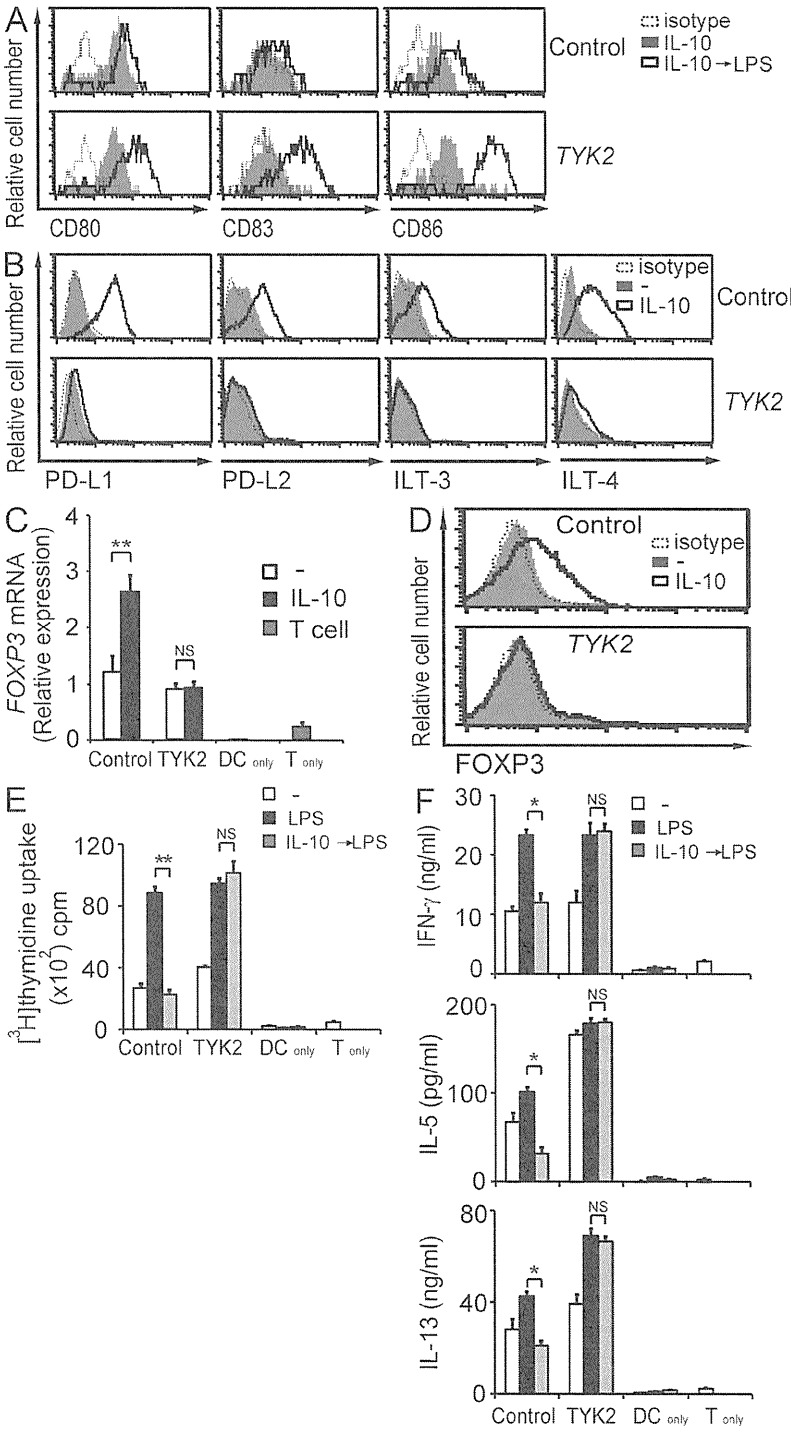

Figure 6. *TYK2*-deficient MoDCs display defective generation of tolerogenic DCs and iT_{reg} cells. (A) Flow cytometric analysis of the CD80, CD83, and CD86 expression on IL-10–DCs (IL-10) and LPS-matured MoDCs after prior treatment with IL-10 (IL-10 → LPS), with cells obtained from a control subject and a patient with *TYK2* deficiency. We show representative histograms from three independent experiments. (B) Flow cytometric analysis of the levels of PD-L1, PD-L2, ILT-3, and ILT-4 in untreated immature MoDCs (−) and IL-10–DCs (IL-10) from a control subject and a *TYK2* deficiency. We show representative histograms from three independent experiments. (C) Q-PCR analysis of *FOXP3* mRNA levels after the co-culture of third-party allogeneic naive $CD4^+$ T cells from a control subject with untreated immature MoDCs (−) or IL-10–DCs (IL-10) from a control subject and a *TYK2*-deficient patient. We show representative data from three independent experiments. (D) Flow cytometric analysis of cytoplasmic FOXP3 protein levels in untreated immature MoDCs (−) and IL-10–DCs (IL-10) from a control subject and a *TYK2*-deficient patient. Isotype-matched control (isotype) antibody staining is indicated by a dashed line. We show representative histograms from three independent experiments. (E) Third-party allogeneic naive $CD4^+$ T cells from control subjects were co-cultured with immature MoDCs (−), LPS-matured MoDCs (LPS), or LPS-matured MoDCs after prior treatment with IL-10 (IL-10 → LPS). The cells were obtained from a control subject and a *TYK2*-deficient patient. After 5 d, proliferation was evaluated by pulsing the cells with 1 µCi (37 kBq) [^{3}H]thymidine for the final 18 h of culture. All samples were evaluated in triplicate. We show representative data from three independent experiments. (F) Cells were cultured as in E, and cytokine levels were evaluated as indicated. All samples were evaluated in triplicate. We show representative data from at least three independent experiments. (C, E, and F) Graphs show mean ± SD. *, $P < 0.05$; **, $P < 0.01$.

The exposure of the skin to allergens induces allergen-specific unresponsiveness, possibly because of the production of IL-10 by keratinocytes (Enk and Katz, 1992; Enk et al., 1993). Langerhans cells and dermal DCs receive IL-10 signal and induce allergen-specific tolerance. This defect in IL-10–mediated tolerance to innocuous environmental antigens may be one of the mechanisms underlying the allergic signs in HIES patients. In humans, we are not certain about the nT_{reg} cell/iT_{reg} cell ratio in the peripheral blood under resting conditions. Our data suggest that most of the T_{reg} cells in the peripheral blood are nT_{reg} cells, which are derived from the thymus and are independent of the IL-10 signal. iT_{reg} cells in the peripheral blood may be a minor population under resting conditions but may play a crucial role in the regulation of antigen-specific allergic reactions.

Human peripheral blood T_{reg} cells suppressed proliferation and Th2 cytokine production by responder T cells stimulated with allergens (Bellinghausen et al., 2003; Grindebacke et al., 2004; Ling et al., 2004). $CD4^+$ T cells cultured with IL-10–DCs have antigen-specific iT_{reg} cell activity (Steinbrink et al., 2002). In vitro experiments suggested that the suppression is dependent on cell to cell contact between iT_{reg} cells and responder T cells and is not mediated by soluble factors. In this study, we found that the generation of $FOXP3^+$ iT_{reg} cells by

Published February 7, 2011

IL-10–DCs was impaired in HIES patients. Evidence is accumulating to suggest that interactions between tolerogenic DCs and T_{reg} cells play an important role in the maintenance of immune tolerance against self-antigens and innocuous environmental antigens (Yamazaki et al., 2006a; Hubert et al., 2007). $CD4^+CD25^+$ T_{reg} cell populations can expand in the presence of DCs with intact suppressive activity in vitro and in vivo (Yamazaki et al., 2006b). In addition to the IL-10 signal provided by the cells sensing innocuous environmental antigens, the IL-10–mediated positive feedback loop between tolerogenic DCs and iT_{reg} cells is probably impaired in HIES patients, and this may also constitute one of the mechanisms underlying the atopic signs in HIES patients.

A large number of clinical studies have demonstrated that IL-10 is involved in the molecular pathogenesis of atopic disorders in humans. The frequency of allergen-specific, IL-10–secreting T cells is significantly higher in nonatopic individuals than in atopic patients (Akdis et al., 2004). IL-10 levels are inversely correlated with the severity of human allergic diseases (Borish et al., 1996; Lim et al., 1998). Furthermore, allergen-specific immunotherapies increase IL-10 synthesis by T cells (Francis et al., 2003; Vissers et al., 2004). All of these findings suggest that IL-10 plays a key role in the control of atopic diseases in humans.

In contrast, mice lacking IL-10 or the IL-10 receptor develop spontaneous inflammation in the large intestine (Kühn et al., 1993; Davidson et al., 1996; Spencer et al., 1998). Mice with a T_{reg} cell–specific IL-10 deficiency also display inflammation of surfaces in contact with the environment such as the colon, lungs, and skin (Rubtsov et al., 2008). In humans, mutations in the genes encoding IL-10 receptor subunits have been found in patients with early-onset enterocolitis (Glocker et al., 2009). Thus, a lack of IL-10 signaling results in enterocolitis in both humans and mice. Interestingly, in patients with HIES, immune responses to innocuous environmental antigens are limited to the skin, with no marked increase in the frequency of enterocolitis. One possible reason for this discrepancy is the existence of a partial, as opposed to complete, IL-10 signaling deficiency in *STAT3* patients, creating a situation resembling T_{reg} cell–specific IL-10 deficiency. An alternative nonmutually exclusive explanation is that, in addition to the IL-10 signaling defect, *STAT3* patients have defective Th17 cell development (de Beaucoudrey et al., 2008; Ma et al., 2008; Milner et al., 2008; Renner et al., 2008; Minegishi et al., 2009). The combination of Th17 cell deficiency and IL-10 signaling may result in allergic signs but prevent the development of enterocolitis (Brand, 2009).

T_{reg} cells mediate peripheral tolerance and play a central role in determining several immunopathologies, including autoimmunity, chronic infections, tumor development, and allergies (Hawrylowicz and O'Garra, 2005). $FOXP3^+$ T_{reg} cells are involved in protecting humans against allergic diseases, as patients with IPEX syndrome suffer from allergic symptoms (Bennett et al., 2001; Wildin et al., 2001). PBMCs from atopic patients proliferate more extensively and produce more Th2 cytokines in response to allergens than do PBMCs from nonatopic healthy individuals (Taams et al., 2002; Ling et al., 2004). However, patients with atopic dermatitis have normal numbers of T_{reg} cells in the periphery with normal suppressive activity (Ou et al., 2004). These results suggest that iT_{reg} cells may be more important than nT_{reg} cells in controlling atopic dermatitis. Consistent with this hypothesis, a recent study using two mouse strains, one capable of generating iT_{reg} cells but incapable of generating nT_{reg} cells and the other unable to generate either iT_{reg} or nT_{reg} cells, suggested that iT_{reg} cells controlled allergic inflammation against innocuous environmental allergens, whereas nT_{reg} cells did not (Curotto de Lafaille et al., 2008).

TGF-β1 is the other crucial inhibitory cytokine regulating lymphocyte homeostasis, inhibiting Th1 and Th2 cell responses and promoting the differentiation of iT_{reg} cells (Li et al., 2006). One previous study suggested that STAT3 might be involved in transduction of the TGF-β1 signal (Ohkawara et al., 2004), but we detected no impairment of TGF-β1 signaling in DCs from *STAT3* patients. Unexpectedly, we found that TGF-β1 and IL-10–DCs operated synergistically to up-regulate FOXP3 expression in naive $CD4^+$ T cells. This suggests that the defective generation of IL-10–DCs may have a far-reaching impact on the induction of iT_{reg} cells in HIES patients.

We provide in this study the first demonstration that an IL-10 signaling defect leads to the impairment of tolerogenic DC and iT_{reg} cell production in the HIES. These results suggest that the defect in tolerogenic DC and iT_{reg} cell production, even in the presence of normal nT_{reg} cells, may contribute to the development of complex clinical manifestations, including allergic inflammation in HIES patients. Furthermore, a unique combination of defective Th17 differentiation and iT_{reg} cell generation may culminate in the development of atopic dermatitis but not enterocolitis in HIES patients.

MATERIALS AND METHODS

Patients. All *STAT3* patients enrolled in this study had typical clinical findings associated with HIES and a National Institutes of Health score >40 points (Table I; Grimbacher et al., 1999). The diagnosis was confirmed by the identification of mutations in the *STAT3* gene. The patient with *TYK2* deficiency has been described elsewhere (Minegishi et al., 2006). The study was approved by the Tokyo Medical and Dental University Ethics Committee, and written informed consent was obtained from all patients. Control individuals were nonatopic, age-matched, and equivalent in sex distribution to HIES patients. All of the patients and control subjects were in a healthy state when their blood samples were collected.

Antibodies, cytokines, and peptides. We used mAbs against CD4 (RPA-T4), CD14 (M5E2), CD11c (B-ly6), CD123 (9F5), HLA-DR (TU36), CD25 (M-A251), CD62L (Dreg 56), CD1a, (HI149), CD80 (L307.4), CD86 (2331), CD83 (HB15e), PD-L1 (MIH1), PD-L2 (MIH18), FOXP3 (259D/C7), and CTLA-4 (CD152; BNI3), a Lin cocktail (antibodies against CD3 [SK7], CD14 [MΦP9], CD16 [3G8], CD19 [SJ25C1], CD20 [L27], and CD56 [NCAM16.2]), and mAbs against IFN-γ (4S.B3) and IL-4 (8D4-8), neutralizing mAbs against IFN-γ (B27), IL-4 (MP4-25D2), and isotype-matched control mAbs, all of which were purchased from BD. We obtained antibodies against ILT-3 (CD85K; 293623), ILT-4 (CD85d; 287219), LAP (latency-associated peptide; TGF-β1; 27235), and GITR (TNFRSF18; 110416) from R&D Systems. Anti–ICOS-L antibody (MIH12) was obtained from eBioscience. Anti-CD304 (BDCA-4) antibody (AD5-17F6) was obtained

JEM Published February 7, 2011

Table I. Characteristics of HIES patients

Patient	Age	Sex	Mutation	Domain	Highest IgE	NIH score															
						Total points	Skin abscess	Pneumonia	Eosinophilia	Newborn rash	Eczema	URI	Candidiasis	Serious infection	Lung abnormality	Face	Nasal width	Retained teeth	Scoliosis	Fracture	Hyperextensibility	High palate
	yr				*IU/ml*																
STAT3-1	23	F	ΔV463	DNA binding	17,500	58	2	8	0	4	2	0	0	0	8	5	3	8	4	0	4	0
STAT3-2	11	F	R382W	DNA binding	97,900	66	8	8	6	4	4	2	1	0	8	2	1	8	0	0	4	0
STAT3-3	24	M	ΔV463	DNA binding	62,000	56	8	0	6	4	4	0	4	4	8	5	1	0	0	0	0	2
STAT3-4	13	M	R382Q	DNA binding	11,600	41	8	8	0	4	4	0	0	4	0	2	1	0	0	0	0	0
STAT3-5	16	F	H437Y	DNA binding	50,600	44	8	4	6	4	4	0	0	0	0	5	3	0	0	0	0	0
STAT3-6	23	F	S636F	SH2	25,400	68	8	8	0	4	2	2	4	0	6	5	3	8	0	4	4	0
STAT3-7	49	F	G618D	SH2	21,300	53	8	8	0	4	4	0	0	4	8	2	1	0	0	4	0	0
STAT3-8	34	M	Δ371-380	DNA binding	12,300	53	8	0	0	4	4	0	4	4	0	5	3	1	0	4	4	2
TYK2-1	23	M	Frame shift	NA	2,100	48	8	8	3	4	4	2	1	8	0	0	0	0	0	0	0	0

NA, not applicable. Possible HIES patients are evaluated by the National Institutes of Health (NIH) scoring system. If the total points of NIH score are >40 points, the patient is considered as HIES clinically. NIH score is defined as follows. If the highest serum IgE level is >2,000 IU/ml, the patient scores 10 points. Skin abscess: 8 points indicate more than four, and 2 points indicate one or two episodes of skin abscess in lifetime. Pneumonia: 8 points indicate more than three, and 4 points indicate two episodes of pneumonia in lifetime. Eosinophilia: 6 points indicate >800 eosinophils/μl, and 3 points indicate 700–800 eosinophils/μl of blood (700/μl = 1 SD and 800/μl = 2 SD above the mean value from normal individuals). Newborn rash: 4 points indicate newborn rash is present. Eczema: 4 points indicate eczema is severe, and 2 points indicate eczema is moderate in worst stage. Upper respiratory infections (URI): 2 points indicate the patient sufferers from upper respiratory infections six to four times, 1 point indicates three times per year. Candidiasis: 4 points indicate the patient has systemic candidiasis, and 1 point indicates oral candidiasis. Serious infections: 8 points indicate the patient has episodes of fatal and serious infection, and 4 points indicate the patient has an episode of serious infection. Lung abnormality: 8 points indicate the patient has pneumatocele, and 6 points indicate the patient has bronchiectasis. Face: 5 points indicate the patient has typical characteristic facial appearance, and 2 points indicate mild characteristic facial appearance. Nasal width: 3 points indicate the patient has nasal width of >2 SD, and 1 point indicates nasal width with 1–2 SD. Retained teeth: 8 points indicate the patient has more than three retained primary teeth, and 1 point indicates the patient has one retained primary tooth. Scoliosis: 4 points indicate the patient has scoliosis of 15–20°, and 2 points indicate scoliosis of 10–14°. Fracture: 4 points indicate the patient has one or two episodes of fracture with minor trauma. Hyperextensibility: 4 points indicate the patient has hyperextensible joints. High palate: 2 points indicate the patient has a high palate. In all items, 0 points indicate the finding is absent. None of the patients have lymphoma or midline anomaly.

Published February 7, 2011

from Miltenyi Biotec. Recombinant human (rh) GM-CSF, IL-4, IFN-γ, IL-10, and TGF-β1 were purchased from PeproTech. Neutralizing PD-L1 peptide was obtained from Abcam, and an irrelevant peptide was used as a negative control.

PBMCs and naive CD4$^+$ T cell culture. PBMCs were isolated by Ficoll density gradient centrifugation (Histopaque-1077; Sigma-Aldrich). PBMCs were cultured in 96-well plates in RPMI 1640 medium supplemented with 10% fetal bovine serum, 200 mM L-glutamine, 100 mM sodium pyruvate, nonessential amino acids, minimal essential medium vitamins (all from Invitrogen), 50 U/50 μg/ml penicillin/streptomycin (Nacalai Tesque), and 50 μM mercaptoethanol. Cultures were stimulated with a 1:100 (vol/vol) dilution of anti-CD3/CD28 mAb–coated beads from Invitrogen. For some experiments, the following mAbs and cytokines were added: 10 ng/ml rhIFN-γ, 10 ng/ml rhIL-4, and neutralizing antibodies against 10 μg/ml IFN-γ and 10 μg/ml IL-4.

T_{reg} cell purification and functional assay. Total CD4$^+$ T cells were isolated with the CD4$^+$ T cell isolation kit (BD). The cells were stained for sorting with antibodies against CD4, CD25, and CD62L. All mAbs were used after dialysis to remove sodium azide (Baecher-Allan et al., 2006). CD4$^+$CD25$^-$CD62L^{hi} responder T cells and CD4$^+$CD25$^+$CD62L^{hi} T_{reg} cell populations were isolated by sorting with a cell sorter (Moflo; Beckman Coulter). In the postsort analysis, the resulting cell preparation was found to be to >99% purity. Co-culture was set up as follows: 1.25×10^4 responder T cells and 1.25×10^3 T_{reg} cells were co-cultured for 5 d with a 1:100 (vol/vol) dilution of magnetic beads coated with antibodies against CD3/CD28. Responder T cells were used as a negative control. Proliferation was assessed by adding 1 μCi (37 kBq) [^{3}H]thymidine (methyl-[^{3}H]thymidine; ICN Biomedicals) to the culture medium for the final 18 h.

Isolation of primary DCs. Primary DCs were obtained by the enrichment using a human DC enrichment set (BD) and cell sorting with FACS Aria II (BD): cDCs as Lin$^-$HLA-DR$^+$ CD11c$^+$CD304$^-$ cells and pDCs as Lin$^-$HLA-DR$^+$CD11c$^-$CD304$^+$ cells. In the postsort analysis, the resulting cell preparation was to >99% purity.

In vitro generation of MoDCs. CD14$^+$ monocytes were isolated from PBMCs with immunomagnetic beads (BD) at a purity of >98%. Monocytes were cultured in the presence of 50 ng/ml GM-CSF and 10 ng/ml IL-4 for 5 d. For differentiation into mature DCs, immature DCs were stimulated on day 5 with 100 ng/ml LPS (O55:B5; Sigma-Aldrich). For the generation of tolerogenic DCs, 100 ng/ml IL-10 was added to the culture on day 3. Nonadherent DCs on day 7 were used for T cell stimulation.

Allogeneic naive CD4$^+$ T cell proliferation assay. Naive CD4$^+$ T cells were negatively selected from PBMCs through the depletion of CD8, CD11b, CD16, CD19, CD36, CD41a, CD45RO, CD56, CD123, γδ-TCR, and glycophorin A–positive cells, with antibody-coated paramagnetic microbeads (naive CD4$^+$ T cell isolation kit from BD), according to the manufacturer's protocol. The purity of the naive CD4$^+$ T cell preparation exceeded 95%. For proliferation assays, 10^5 naive CD4$^+$ T cells were co-cultured in 96-well round-bottomed plates, in triplicate, with 10^4 allogeneic DCs. After 5 d, the cells were pulsed with 1 μCi (37 kBq) per well of [^{3}H]thymidine for 18 h, and [^{3}H]thymidine incorporation was evaluated with a β counter (model 1450; PerkinElmer).

iT_{reg} cell preparation and functional evaluation. Naive CD4$^+$ T cells were obtained from PBMCs with the naive CD4$^+$ T cell isolation kit. We obtained CD4$^+$CD25$^-$ responder T cells by depleting the CD25$^+$ cells with magnetic beads coated with an antibody against CD25 (BD). The resulting cell preparation was >95% pure. We obtained iT_{reg} cells by setting up cocultures as described for the Allogeneic naive CD4$^+$ T cell proliferation assay and purifying CD4$^+$CD25$^+$ cells after 3 d with immunomagnetic beads. CD4$^+$CD25$^+$ iT_{reg} cells were co-cultured with CFSE-labeled autologous CD4$^+$CD25$^-$ responder T cells in 96-well round-bottomed plates containing a 1:100 (vol/vol) dilution of anti-CD3/CD28 mAb beads. After 5 d, the proliferation of the CFSE-labeled CD4$^+$CD25$^-$ T cells was assessed by flow cytometry.

Flow cytometric analysis. Cells were analyzed on a FACSCalibur or FACSCanto II machine (BD) using CellQuest or FACSDiva software (BD).

Mannose receptor–mediated endocytosis. 1 mg/ml FITC–dextran (Sigma-Aldrich) was incubated with 10^5 cells at 37°C or 4°C for 2 h. FITC-dextran uptake was stopped by adding ice-cold PBS, and the cells were then thoroughly washed in a refrigerated centrifuge. Samples were then subjected to flow cytometry. The level of antigen uptake by DCs was assessed as the difference between the test (37°C) and control (4°C) values for each sample.

Cytokine ELISA. For cytokine determinations, the culture supernatant was stored at −80°C until use, and the amounts of IFN-γ, TNF, IL-5, IL-6, IL-10, IL-12p40, and IL-13 present were then determined by ELISA, according to the kit manufacturer's instructions (BD).

Intracellular staining. Naive CD4$^+$ T cells were cultured with plate-bound antibodies against CD3 and CD28 in Th1 conditions, IFN-γ plus antibody against IL-4 in Th2 conditions, or IL-4 and antibody against IFN-γ, and the cells were then fixed and permeabilized (Cytofix/Cytoperm reagents; BD) and stained with mAbs against CD4, IFN-γ, and IL-4, according to the manufacturer's instructions (BD). CTLA-4 staining was performed after Cytofix/Cytoperm treatment.

FOXP3 intracellular staining. Naive CD4$^+$ T cells co-cultured with untreated DCs or IL-10–DCs were fixed and permeabilized with the human FOXP3 buffer set (BD) and stained with mAb against FOXP3.

RNA isolation and real-time quantitative RT-PCR (Q-PCR). Cells were harvested for total RNA isolation with the Fastpure RNA kit (Takara Bio Inc.). Total RNA was reverse transcribed with Primescript RT (Takara Bio Inc.). An aliquot of the RT products was used as a template for real-time PCR with SYBR green Mastermix (Takara Bio Inc.) on an Mx3005P thermocycler (Agilent Technologies) with SYBR green I dye as the amplicon detector and ROX as the passive reference. The gene for HPRT (hypoxanthine phosphoribosyltransferase) was amplified as an endogenous reference. Quantification was achieved by both the standard curve and comparative ΔΔCT methods.

Data analysis. Data are expressed as means ± the SD. Unpaired *t* tests or analysis of variance was used for statistical analysis. P-values <0.05 were considered significant (*, $P < 0.05$; **, $P < 0.01$; and ***, $P < 0.001$).

Online supplemental material. Fig. S1 shows normal Th1 and Th2 differentiation from naive CD4$^+$ T cells but increased Th2 cytokine production from activated T cells in PBMCs of *STAT3* patients. Fig. S2 shows that MoDC differentiation in vitro and TGF-β1 signaling in MoDCs are intact in *STAT3* patients. Fig. S3 shows that IL-10 treatment does not impair the differentiation of MoDCs, but down-regulation of CD80, CD83, and CD86 is defective in MoDCs from *STAT3* patients. Fig. S4 shows that suppression of proliferation by IL-10 pretreatment is impaired in MoDCs from *STAT3* patients. Fig. S5 shows that up-regulation of FOXP3, CTLA-4, and GITR is impaired in iT_{reg} cells co-cultured with patient IL-10–DCs. Fig. S6 shows that MoDCs from *STAT3* patients produce equivalent amounts of TGF-β1. Fig. S7 shows the characterization of primary DCs and MoDCs from the patient with *TYK2* deficiency. Online supplemental material is available at http://www.jem.org/cgi/content/full/jem.20100799/DC1.

We thank Ms. S. Miyakoshi for assistance with cell sorting with Moflo.

This work is supported by Grants-in-Aid from the Japanese Ministry of Education, Culture, Sports, Science and Technology (22021015 and 22390205),

Published February 7, 2011

JEM

Japan Science and Technology Agency, Core Research for Evolutional Science and Technology, Research on Intractable Diseases from the Ministry of Health, Labour and Welfare, the Uehara Foundation, the Naito Foundation, the Takeda Science Foundation, and the Mitsubishi Foundation.

The authors have no conflicting financial interests.

Submitted: 22 April 2010
Accepted: 11 January 2011

REFERENCES

Akdis, C.A., and M. Akdis. 2009. Mechanisms and treatment of allergic disease in the big picture of regulatory T cells. *J. Allergy Clin. Immunol.* 123:735–746. doi:10.1016/j.jaci.2009.02.030

Akdis, M., J. Verhagen, A. Taylor, F. Karamloo, C. Karagiannidis, R. Crameri, S. Thunberg, G. Deniz, R. Valenta, H. Fiebig, et al. 2004. Immune responses in healthy and allergic individuals are characterized by a fine balance between allergen-specific T regulatory 1 and T helper 2 cells. *J. Exp. Med.* 199:1567–1575. doi:10.1084/jem.20032058

Akira, S. 2000. Roles of STAT3 defined by tissue-specific gene targeting. *Oncogene.* 19:2607–2611. doi:10.1038/sj.onc.1203478

Amsen, D., A. Antov, and R.A. Flavell. 2009. The different faces of Notch in T-helper-cell differentiation. *Nat. Rev. Immunol.* 9:116–124. doi:10.1038/nri2488

Avery, D.T., E.K. Deenick, C.S. Ma, S. Suryani, N. Simpson, G.Y. Chew, T.D. Chan, U. Palendira, J. Bustamante, S. Boisson-Dupuis, et al. 2010. B cell–intrinsic signaling through IL-21 receptor and STAT3 is required for establishing long-lived antibody responses in humans. *J. Exp. Med.* 207:155–171. doi:10.1084/jem.20091706

Baecher-Allan, C., E. Wolf, and D.A. Hafler. 2006. MHC class II expression identifies functionally distinct human regulatory T cells. *J. Immunol.* 176:4622–4631.

Banchereau, J., F. Briere, C. Caux, J. Davoust, S. Lebecque, Y.J. Liu, B. Pulendran, and K. Palucka. 2000. Immunobiology of dendritic cells. *Annu. Rev. Immunol.* 18:767–811. doi:10.1146/annurev.immunol.18.1.767

Bellinghausen, I., B. Klostermann, J. Knop, and J. Saloga. 2003. Human CD4+CD25+ T cells derived from the majority of atopic donors are able to suppress TH1 and TH2 cytokine production. *J. Allergy Clin. Immunol.* 111:862–868. doi:10.1067/mai.2003.1412

Bennett, C.L., J. Christie, F. Ramsdell, M.E. Brunkow, P.J. Ferguson, L. Whitesell, T.E. Kelly, F.T. Saulsbury, P.F. Chance, and H.D. Ochs. 2001. The immune dysregulation, polyendocrinopathy, enteropathy, X-linked syndrome (IPEX) is caused by mutations of FOXP3. *Nat. Genet.* 27:20–21. doi:10.1038/83713

Bettelli, E., Y. Carrier, W. Gao, T. Korn, T.B. Strom, M. Oukka, H.L. Weiner, and V.K. Kuchroo. 2006. Reciprocal developmental pathways for the generation of pathogenic effector TH17 and regulatory T cells. *Nature.* 441:235–238. doi:10.1038/nature04753

Borish, L., A. Aarons, J. Rumbyrt, P. Cvietusa, J. Negri, and S. Wenzel. 1996. Interleukin-10 regulation in normal subjects and patients with asthma. *J. Allergy Clin. Immunol.* 97:1288–1296. doi:10.1016/S0091-6749(96)70197-5

Brand, S. 2009. Crohn's disease: Th1, Th17 or both? The change of a paradigm: new immunological and genetic insights implicate Th17 cells in the pathogenesis of Crohn's disease. *Gut.* 58:1152–1167. doi:10.1136/gut.2008.163667

Chen, W., W. Jin, N. Hardegen, K.J. Lei, L. Li, N. Marinos, G. McGrady, and S.M. Wahl. 2003. Conversion of peripheral $CD4^+CD25^-$ naive T cells to $CD4^+CD25^+$ regulatory T cells by TGF-β induction of transcription factor *Foxp3*. *J. Exp. Med.* 198:1875–1886. doi:10.1084/jem.20030152

Coombes, J.L., K.R. Siddiqui, C.V. Arancibia-Cárcamo, J. Hall, C.M. Sun, Y. Belkaid, and F. Powrie. 2007. A functionally specialized population of mucosal $CD103^+$ DCs induces $Foxp3^+$ regulatory T cells via a TGF-β– and retinoic acid–dependent mechanism. *J. Exp. Med.* 204:1757–1764. doi:10.1084/jem.20070590

Corinti, S., C. Albanesi, A. la Sala, S. Pastore, and G. Girolomoni. 2001. Regulatory activity of autocrine IL-10 on dendritic cell functions. *J. Immunol.* 166:4312–4318.

Curotto de Lafaille, M.A., S. Muriglan, M.J. Sunshine, Y. Lei, N. Kutchukhidze, G.C. Furtado, A.K. Wensky, D. Olivares-Villagómez, and J.J. Lafaille. 2001. Hyper immunoglobulin E response in mice with monoclonal populations of B and T lymphocytes. *J. Exp. Med.* 194:1349–1359. doi:10.1084/jem.194.9.1349

Curotto de Lafaille, M.A., N. Kutchukhidze, S. Shen, Y. Ding, H. Yee, and J.J. Lafaille. 2008. Adaptive Foxp3+ regulatory T cell-dependent and -independent control of allergic inflammation. *Immunity.* 29:114–126. doi:10.1016/j.immuni.2008.05.010

Davidson, N.J., M.W. Leach, M.M. Fort, L. Thompson-Snipes, R. Kühn, W. Müller, D.J. Berg, and D.M. Rennick. 1996. T helper cell 1-type CD4+ T cells, but not B cells, mediate colitis in interleukin 10-deficient mice. *J. Exp. Med.* 184:241–251. doi:10.1084/jem.184.1.241

de Beaucoudrey, L., A. Puel, O. Filipe-Santos, A. Cobat, P. Ghandil, M. Chrabieh, J. Feinberg, H. von Bernuth, A. Samarina, L. Jannière, et al. 2008. Mutations in STAT3 and IL12RB1 impair the development of human IL-17-producing T cells. *J. Exp. Med.* 205:1543–1550. doi:10.1084/jem.20080321

Dillon, S.R., C. Sprecher, A. Hammond, J. Bilsborough, M. Rosenfeld-Franklin, S.R. Presnell, H.S. Haugen, M. Maurer, B. Harder, J. Johnston, et al. 2004. Interleukin 31, a cytokine produced by activated T cells, induces dermatitis in mice. *Nat. Immunol.* 5:752–760. doi:10.1038/ni1084

Enk, A.H., and S.I. Katz. 1992. Early molecular events in the induction phase of contact sensitivity. *Proc. Natl. Acad. Sci. USA.* 89:1398–1402. doi:10.1073/pnas.89.4.1398

Enk, A.H., V.L. Angeloni, M.C. Udey, and S.I. Katz. 1993. Inhibition of Langerhans cell antigen-presenting function by IL-10. A role for IL-10 in induction of tolerance. *J. Immunol.* 151:2390–2398.

Fontenot, J.D., M.A. Gavin, and A.Y. Rudensky. 2003. Foxp3 programs the development and function of CD4+CD25+ regulatory T cells. *Nat. Immunol.* 4:330–336. doi:10.1038/ni904

Francis, J.N., S.J. Till, and S.R. Durham. 2003. Induction of IL-10+ CD4+CD25+ T cells by grass pollen immunotherapy. *J. Allergy Clin. Immunol.* 111:1255–1261. doi:10.1067/mai.2003.1570

Francisco, L.M., V.H. Salinas, K.E. Brown, V.K. Vanguri, G.J. Freeman, V.K. Kuchroo, and A.H. Sharpe. 2009. PD-L1 regulates the development, maintenance, and function of induced regulatory T cells. *J. Exp. Med.* 206:3015–3029. doi:10.1084/jem.20090847

Glocker, E.O., D. Kotlarz, K. Boztug, E.M. Gertz, A.A. Schäffer, F. Noyan, M. Perro, J. Diestelhorst, A. Allroth, D. Murugan, et al. 2009. Inflammatory bowel disease and mutations affecting the interleukin-10 receptor. *N. Engl. J. Med.* 361:2033–2045. doi:10.1056/NEJMoa0907206

Grimbacher, B., A.A. Schäffer, S.M. Holland, J. Davis, J.I. Gallin, H.L. Malech, T.P. Atkinson, B.H. Belohradsky, R.H. Buckley, F. Cossu, et al. 1999. Genetic linkage of hyper-IgE syndrome to chromosome 4. *Am. J. Hum. Genet.* 65:735–744. doi:10.1086/302547

Grimbacher, B., S.M. Holland, and J.M. Puck. 2005. Hyper-IgE syndromes. *Immunol. Rev.* 203:244–250. doi:10.1111/j.0105-2896.2005.00228.x

Grindebacke, H., K. Wing, A.C. Andersson, E. Suri-Payer, S. Rak, and A. Rudin. 2004. Defective suppression of Th2 cytokines by CD4CD25 regulatory T cells in birch allergics during birch pollen season. *Clin. Exp. Allergy.* 34:1364–1372. doi:10.1111/j.1365-2222.2004.02067.x

Hammad, H., and B.N. Lambrecht. 2008. Dendritic cells and epithelial cells: linking innate and adaptive immunity in asthma. *Nat. Rev. Immunol.* 8:193–204. doi:10.1038/nri2275

Harrington, L.E., R.D. Hatton, P.R. Mangan, H. Turner, T.L. Murphy, K.M. Murphy, and C.T. Weaver. 2005. Interleukin 17-producing CD4+ effector T cells develop via a lineage distinct from the T helper type 1 and 2 lineages. *Nat. Immunol.* 6:1123–1132. doi:10.1038/ni1254

Hawrylowicz, C.M., and A. O'Garra. 2005. Potential role of interleukin-10-secreting regulatory T cells in allergy and asthma. *Nat. Rev. Immunol.* 5:271–283. doi:10.1038/nri1589

Holland, S.M., F.R. DeLeo, H.Z. Elloumi, A.P. Hsu, G. Uzel, N. Brodsky, A.F. Freeman, A. Demidowich, J. Davis, M.L. Turner, et al. 2007. STAT3 mutations in the hyper-IgE syndrome. *N. Engl. J. Med.* 357:1608–1619. doi:10.1056/NEJMoa073687

Hubert, P., N. Jacobs, J.H. Caberg, J. Boniver, and P. Delvenne. 2007. The cross-talk between dendritic and regulatory T cells: good or evil? *J. Leukoc. Biol.* 82:781–794. doi:10.1189/jlb.1106694

Ivanov, I.I., B.S. McKenzie, L. Zhou, C.E. Tadokoro, A. Lepelley, J.J. Lafaille, D.J. Cua, and D.R. Littman. 2006. The orphan nuclear receptor RORgammat directs the differentiation program of proinflammatory IL-17+ T helper cells. *Cell.* 126:1121–1133. doi:10.1016/j.cell.2006.07.035

Kakkar, R., and R.T. Lee. 2008. The IL-33/ST2 pathway: therapeutic target and novel biomarker. *Nat. Rev. Drug Discov.* 7:827–840. doi:10.1038/nrd2660

Kapsenberg, M.L. 2003. Dendritic-cell control of pathogen-driven T-cell polarization. *Nat. Rev. Immunol.* 3:984–993. doi:10.1038/nri1246

Keir, M.E., M.J. Butte, G.J. Freeman, and A.H. Sharpe. 2008. PD-1 and its ligands in tolerance and immunity. *Annu. Rev. Immunol.* 26:677–704. doi:10.1146/annurev.immunol.26.021607.090331

Kühn, R., J. Löhler, D. Rennick, K. Rajewsky, and W. Müller. 1993. Interleukin-10-deficient mice develop chronic enterocolitis. *Cell.* 75:263–274. doi:10.1016/0092-8674(93)80068-P

Li, M.O., Y.Y. Wan, S. Sanjabi, A.K. Robertson, and R.A. Flavell. 2006. Transforming growth factor-beta regulation of immune responses. *Annu. Rev. Immunol.* 24:99–146. doi:10.1146/annurev.immunol.24.021605.090737

Lim, S., E. Crawley, P. Woo, and P.J. Barnes. 1998. Haplotype associated with low interleukin-10 production in patients with severe asthma. *Lancet.* 352:113. doi:10.1016/S0140-6736(98)85018-6

Lin, W., N. Truong, W.J. Grossman, D. Haribhai, C.B. Williams, J. Wang, M.G. Martín, and T.A. Chatila. 2005. Allergic dysregulation and hyperimmunoglobulinemia E in Foxp3 mutant mice. *J. Allergy Clin. Immunol.* 116:1106–1115. doi:10.1016/j.jaci.2005.08.046

Ling, E.M., T. Smith, X.D. Nguyen, C. Pridgeon, M. Dallman, J. Arbery, V.A. Carr, and D.S. Robinson. 2004. Relation of CD4+CD25+ regulatory T-cell suppression of allergen-driven T-cell activation to atopic status and expression of allergic disease. *Lancet.* 363:608–615. doi:10.1016/S0140-6736(04)15592-X

Lloyd, C.M., and C.M. Hawrylowicz. 2009. Regulatory T cells in asthma. *Immunity.* 31:438–449. doi:10.1016/j.immuni.2009.08.007

Ma, C.S., G.Y. Chew, N. Simpson, A. Priyadarshi, M. Wong, B. Grimbacher, D.A. Fulcher, S.G. Tangye, and M.C. Cook. 2008. Deficiency of Th17 cells in hyper IgE syndrome due to mutations in *STAT3*. *J. Exp. Med.* 205:1551–1557. doi:10.1084/jem.20080218

Milner, J.D., J.M. Brenchley, A. Laurence, A.F. Freeman, B.J. Hill, K.M. Elias, Y. Kanno, C. Spalding, H.Z. Elloumi, M.L. Paulson, et al. 2008. Impaired T(H)17 cell differentiation in subjects with autosomal dominant hyper-IgE syndrome. *Nature.* 452:773–776. doi:10.1038/nature06764

Minegishi, Y. 2009. Hyper-IgE syndrome. *Curr. Opin. Immunol.* 21:487–492. doi:10.1016/j.coi.2009.07.013

Minegishi, Y., M. Saito, T. Morio, K. Watanabe, K. Agematsu, S. Tsuchiya, H. Takada, T. Hara, N. Kawamura, T. Ariga, et al. 2006. Human tyrosine kinase 2 deficiency reveals its requisite roles in multiple cytokine signals involved in innate and acquired immunity. *Immunity.* 25:745–755. doi:10.1016/j.immuni.2006.09.009

Minegishi, Y., M. Saito, S. Tsuchiya, I. Tsuge, H. Takada, T. Hara, N. Kawamura, T. Ariga, S. Pasic, O. Stojkovic, et al. 2007. Dominant-negative mutations in the DNA-binding domain of STAT3 cause hyper-IgE syndrome. *Nature.* 448:1058–1062. doi:10.1038/nature06096

Minegishi, Y., M. Saito, M. Nagasawa, H. Takada, T. Hara, S. Tsuchiya, K. Agematsu, M. Yamada, N. Kawamura, T. Ariga, et al. 2009. Molecular explanation for the contradiction between systemic Th17 defect and localized bacterial infection in hyper-IgE syndrome. *J. Exp. Med.* 206:1291–1301. doi:10.1084/jem.20082767

Ohkawara, B., K. Shirakabe, J. Hyodo-Miura, R. Matsuo, N. Ueno, K. Matsumoto, and H. Shibuya. 2004. Role of the TAK1-NLK-STAT3 pathway in TGF-beta-mediated mesoderm induction. *Genes Dev.* 18:381–386. doi:10.1101/gad.1166904

Ou, L.S., E. Goleva, C. Hall, and D.Y. Leung. 2004. T regulatory cells in atopic dermatitis and subversion of their activity by superantigens. *J. Allergy Clin. Immunol.* 113:756–763. doi:10.1016/j.jaci.2004.01.772

Renner, E.D., S. Rylaarsdam, S. Anover-Sombke, A.L. Rack, J. Reichenbach, J.C. Carey, Q. Zhu, A.F. Jansson, J. Barboza, L.F. Schimke, et al. 2008. Novel signal transducer and activator of transcription 3 (STAT3) mutations, reduced T(H)17 cell numbers, and variably defective STAT3 phosphorylation in hyper-IgE syndrome. *J. Allergy Clin. Immunol.* 122:181–187. doi:10.1016/j.jaci.2008.04.037

Rubtsov, Y.P., and A.Y. Rudensky. 2007. TGFbeta signalling in control of T-cell-mediated self-reactivity. *Nat. Rev. Immunol.* 7:443–453. doi:10.1038/nri2095

Rubtsov, Y.P., J.P. Rasmussen, E.Y. Chi, J. Fontenot, L. Castelli, X. Ye, P. Treuting, L. Siewe, A. Roers, W.R. Henderson Jr., et al. 2008. Regulatory T cell-derived interleukin-10 limits inflammation at environmental interfaces. *Immunity.* 28:546–558. doi:10.1016/j.immuni.2008.02.017

Rutella, S., S. Danese, and G. Leone. 2006. Tolerogenic dendritic cells: cytokine modulation comes of age. *Blood.* 108:1435–1440. doi:10.1182/blood-2006-03-006403

Sakaguchi, S., T. Yamaguchi, T. Nomura, and M. Ono. 2008. Regulatory T cells and immune tolerance. *Cell.* 133:775–787. doi:10.1016/j.cell.2008.05.009

Schulz, O., A.D. Edwards, M. Schito, J. Aliberti, S. Manickasingham, A. Sher, and C. Reis e Sousa. 2000. CD40 triggering of heterodimeric IL-12 p70 production by dendritic cells in vivo requires a microbial priming signal. *Immunity.* 13:453–462. doi:10.1016/S1074-7613(00)00045-5

Spencer, S.D., F. Di Marco, J. Hooley, S. Pitts-Meek, M. Bauer, A.M. Ryan, B. Sordat, V.C. Gibbs, and M. Aguet. 1998. The orphan receptor CRF2-4 is an essential subunit of the interleukin 10 receptor. *J. Exp. Med.* 187:571–578. doi:10.1084/jem.187.4.571

Steinbrink, K., E. Graulich, S. Kubsch, J. Knop, and A.H. Enk. 2002. CD4(+) and CD8(+) anergic T cells induced by interleukin-10-treated human dendritic cells display antigen-specific suppressor activity. *Blood.* 99:2468–2476. doi:10.1182/blood.V99.7.2468

Steinman, R.M., D. Hawiger, and M.C. Nussenzweig. 2003. Tolerogenic dendritic cells. *Annu. Rev. Immunol.* 21:685–711. doi:10.1146/annurev.immunol.21.120601.141040

Taams, L.S., M. Vukmanovic-Stejic, J. Smith, P.J. Dunne, J.M. Fletcher, F.J. Plunkett, S.B. Ebeling, G. Lombardi, M.H. Rustin, J.W. Bijlsma, et al. 2002. Antigen-specific T cell suppression by human CD4+CD25+ regulatory T cells. *Eur. J. Immunol.* 32:1621–1630. doi:10.1002/1521-4141(200206)32:6<1621::AID-IMMU1621>3.0.CO;2-Q

Trautmann, A., M. Akdis, D. Kleemann, F. Altznauer, H.U. Simon, T. Graeve, M. Noll, E.B. Bröcker, K. Blaser, and C.A. Akdis. 2000. T cell-mediated Fas-induced keratinocyte apoptosis plays a key pathogenetic role in eczematous dermatitis. *J. Clin. Invest.* 106:25–35. doi:10.1172/JCI9199

Umetsu, D.T., and R.H. DeKruyff. 2006. The regulation of allergy and asthma. *Immunol. Rev.* 212:238–255. doi:10.1111/j.0105-2896.2006.00413.x

Veldhoen, M., R.J. Hocking, C.J. Atkins, R.M. Locksley, and B. Stockinger. 2006. TGFbeta in the context of an inflammatory cytokine milieu supports de novo differentiation of IL-17-producing T cells. *Immunity.* 24:179–189. doi:10.1016/j.immuni.2006.01.001

Vissers, J.L., B.C. van Esch, G.A. Hofman, M.L. Kapsenberg, F.R. Weller, and A.J. van Oosterhout. 2004. Allergen immunotherapy induces a suppressive memory response mediated by IL-10 in a mouse asthma model. *J. Allergy Clin. Immunol.* 113:1204–1210. doi:10.1016/j.jaci.2004.02.041

Wang, Y.H., P. Angkasekwinai, N. Lu, K.S. Voo, K. Arima, S. Hanabuchi, A. Hippe, C.J. Corrigan, C. Dong, B. Homey, et al. 2007. IL-25 augments type 2 immune responses by enhancing the expansion and functions of TSLP-DC–activated Th2 memory cells. *J. Exp. Med.* 204:1837–1847. doi:10.1084/jem.20070406

Wildin, R.S., F. Ramsdell, J. Peake, F. Faravelli, J.L. Casanova, N. Buist, E. Levy-Lahad, M. Mazzella, O. Goulet, L. Perroni, et al. 2001. X-linked neonatal diabetes mellitus, enteropathy and endocrinopathy syndrome is the human equivalent of mouse scurfy. *Nat. Genet.* 27:18–20. doi:10.1038/83707

Yamazaki, S., K. Inaba, K.V. Tarbell, and R.M. Steinman. 2006a. Dendritic cells expand antigen-specific Foxp3+ CD25+ CD4+ regulatory T cells including suppressors of alloreactivity. *Immunol. Rev.* 212:314–329. doi:10.1111/j.0105-2896.2006.00422.x

Yamazaki, S., M. Patel, A. Harper, A. Bonito, H. Fukuyama, M. Pack, K.V. Tarbell, M. Talmor, J.V. Ravetch, K. Inaba, and R.M. Steinman. 2006b. Effective expansion of alloantigen-specific Foxp3+ CD25+ CD4+ regulatory T cells by dendritic cells during the mixed leukocyte reaction. *Proc. Natl. Acad. Sci. USA.* 103:2758–2763. doi:10.1073/pnas.0510606103

Zheng, S.G., J. Wang, P. Wang, J.D. Gray, and D.A. Horwitz. 2007. IL-2 is essential for TGF-beta to convert naive CD4+CD25- cells to CD25+Foxp3+ regulatory T cells and for expansion of these cells. *J. Immunol.* 178:2018–2027.

Zheng, Y., and A.Y. Rudensky. 2007. Foxp3 in control of the regulatory T cell lineage. *Nat. Immunol.* 8:457–462. doi:10.1038/ni1455

TABLE 2 Details of response to sequential treatments where applicable ($n = 10$)

No.	Severity of disease	First treatment		Second treatment		Third treatment	
1	Severe	Amlodopine	×	Nifedipine	√	–	–
2	Moderate	Amlodopine	×	GTN	×	–	–
3	Moderate	Amlodopine	×	GTN	×	–	–
4	Severe	Nifedipine	×	Amlodopine	×	–	–
5	Severe	Nifedipine	×	Amlodopine	×	GTN	√
6	Moderate	Nifedipine	×	GTN	×	–	
7	Severe	GTN	×	Amlodopine	×	Nifedipine	√
8	Moderate	Nifedipine	×	GTN	√	–	–
9	Severe	Amlodopine	×	Nifedipine	×	GTN	×
10	Moderate	Amlodopine	√	GTN	√	–	–

×: no response/inadequate response; √: response.

Overall, GTN patches were effective in 55% of the treated patients. Efficacy was better than that of nifedipine and amlodipine (33 *vs* 25% response rate, respectively), but small numbers and retrospective analysis does not allow statistical comparison. Response was similar in primary and secondary RP. Children with severe RP had a better response to nifedipine and amlodopine than children with moderate disease. The sub-group with severe disease was more likely to be using a disease-modifying drug, which may have had an impact. However, numbers are too small for any conclusion to be drawn from this.

Application of GTN patches allows removal if adverse events occur. Together with absence of tablets, this may make treatment with GTN attractive in paediatric practice. All patients received Deponit GTN patches. Alternative brands may not have adequate skin adhesion when cut into quarters for this off-license use.

GTN patches, nifedipine and amlodipine offer symptomatic relief for patients with moderate primary/secondary RP. Further studies, including head-to-head trials, are needed to determine if one agent is superior. Meanwhile, GTN patches offer an alternative to oral calcium channel blockers for symptomatic relief of paediatric RP.

Rheumatology key message

- GTN patches are an efficacious treatment option in paediatric RP.

Disclosure statement: The authors have declared no conflicts of interest.

Kapil Gargh[1], Eileen M. Baildam[1], Gavin A. Cleary[1], Michael W. Beresford[1] and Liza J. McCann[1]

[1]*Department of Paediatric Rheumatology, Alder Hey Children's NHS Foundation Trust, Liverpool, UK*
Accepted 20 August 2009
Correspondence to: Liza McCann, Department of Paediatric Rheumatology, Alder Hey Children's NHS Foundation Trust, Eaton Road, Liverpool, L12 2AP, UK.
E-mail: liza.mccann@alderhey.nhs.uk

References

1 Anderson ME, Moore TL, Hollis S, Jayson MIV, King TA, Herrick AL. Digital vascular response to topical glyceryl trinitrate, as measured by laser Doppler imaging, in primary Raynaud's phenomenon and systemic sclerosis. Rheumatology 2002;41:324–28.

2 Franks AG Jr. Topical glyceryl trinitrate as adjunctive treatment in Raynaud's disease. Lancet 1982;1:76–7.

3 Teh LS, Mannig J, Moore T, Tully MP, O'Reilly D, Jayson MIV. Sustained-release transdermal glyceryl trinitrate patches as a treatment for primary and secondary Raynaud's phenomenon. Br J Rheumatol 1995; 34:636–41.

4 Nigrovic PA, Fuhlbrigge RC, Sundel RP. Raynaud's phenomenon in children: a retrospective review of 123 patients. Pediatrics 2003;111:715–21.

5 Coppock JS, Hardman JM, Bacon PA, Woods KL, Kendall MJ. Objective relief of vasospasm by glyceryl trinitrate in secondary Raynaud's phenomenon. Postgrad Med J 1986;62:8–15.

Rheumatology 2010;49:194–196
doi:10.1093/rheumatology/kep315
Advance Access publication 23 October 2009

A case of early-onset sarcoidosis with a six-base deletion in the *NOD2* gene

SIR, We present the first case of early-onset sarcoidosis (EOS, MIM no. 609464) with a six-base deletion in the *NOD2* gene, resulting in the replacement of one amino acid and the deletion of two additional amino acids. All previous mutations reported for EOS and Blau syndrome (BS, MIM no. 186580) were single-base substitutions that resulted in the replacement of a single amino acid [1–3].

The patient was a Japanese male born after an uncomplicated pregnancy and delivery. His family had no symptoms of skin lesions, arthritis or uveitis. At 5 years of age, he was diagnosed with bilateral severe uveitis. He became blind in both eyes during adolescence. He had swollen ankles without pain during childhood,

and developed arthritis in his both knees and ankles at 15 years of age. At 30 years, a skin rash had developed on his extremities after his first BCG vaccination. The skin lesions were scaly erythematous plaques with multiple lichenoid papules and some pigmentation. At the same age, camptodactyly without obvious synovial cysts of the hands was observed, and the deformity in all fingers developed by 35 years. At 41 years, he had low-grade fever for 1 year. He had no pulmonary lesions. His laboratory investigations showed normal white blood cell count, mildly elevated CRP (1.0 mg/dl) and ESR (20 mm/h). A skin biopsy from his left forearm revealed non-caseating granulomas without lymphocyte infiltration. There were no indications of infection by *Mycobacterium*.

The clinical symptoms and pathological findings on the biopsied skin indicated that the patient suffered from EOS. It has been reported that EOS and BS have a common genetic aetiology due to mutations in the *NOD2* gene that cause constitutive Nuclear Factor (NF)-κB activation [4, 5]. Thus we analysed the *NOD2* gene from the patient to look for mutations that might correlate with the pathology of EOS. A written informed consent was obtained from the patient and his families, according to the protocol of the institutional review board of Kyoto University Hospital and in accordance with the Declaration of Helsinki. Genomic sequencing analysis of the patient's *NOD2* gene showed the presence of a heterozygous deletion of six bases in exon 4, which resulted in c.1493_1498delAACTGT, p.E498V, 499–500del (Fig. 1A). The mutation was novel and was not identified in 100 normal controls. A genome alignment of *NOD2* among several species showed that E498, L499 and L500 are conserved from zebrafish to human (Fig. 1B). These data strongly suggested that the identified deletion of six bases in the *NOD2* gene is not a single nucleotide polymorphism (SNP), but is probably responsible for EOS in the patient.

Previous studies report that *NOD2* mutations causing EOS/BS show constitutive activation of NF-κB [6–8]. Therefore, we investigated the level of NF-κB activity associated with the new mutation identified here. First, we confirmed the level of mRNA expression of the mutated allele by subcloning analysis of *NOD2*-cDNA, which showed that the mutated allele was expressed as well as the wild type allele (data not shown). We then evaluated the ability of the *NOD2* mutant to constitutively activate NF-κB by using an *in vitro* reporter system in HEK293T cells transfected with both *NOD2* mutants and NF-κB reporter plasmids (Fig. 1C). The deletion mutant demonstrated almost five times more NF-κB activity than wild type without muramyl dipeptide (MDP) stimulation. Western blot analysis confirmed that NOD2 mutant protein expression was similar to that of wild type (Fig. 1C). Thus, like other mutations of *NOD2* identified previously, the deletion mutant identified here also showed constitutive activation of NF-κB.

The mechanism underlying EOS/BS has not been totally understood, although two pathways downstream from *NOD2* have been identified: NF-κB activation through receptor-interacting protein (RIP) like interacting caspase-like apoptosis regulatory protein kinase (RICK) and MAP kinase activation through the caspase recruitment domain 9 (CARD9) [9]. We previously tested 10 *NOD2* missense mutations that have been identified in our cohort of EOS/BS patients in Japan, and all of them demonstrated constitutive activation of NF-κB [3]. By analysing this newly identified deletion mutant, we have further confirmed the importance of constitutive activation of NF-κB by mutated *NOD2* for the pathogenesis of EOS/BS. We would like to emphasize the

FIG. 1 (**A**) Summary of the mutations identified in our patient. (**B**) NOD2 protein alignment among different species on the mutated amino acids. (**C**) NF-κB reporter assay using the *NOD2* deletion mutant. *In vitro* NF-κB reporter assays were performed as previously described [1, 3, 6, 7]. Mock vector, wild type *NOD2* (WT) and three *NOD2* variants (R334W, C495Y, H496L) derived from EOS/BS patients, were used as controls. Values represent the mean of normalized data (mock without MDP = 1) of triplicate cultures, and error bars indicate S.D. Shown is one representative result of three independent experiments. Protein expression levels of *NOD2* mutants analysed by western blotting are shown in the bottom panel.

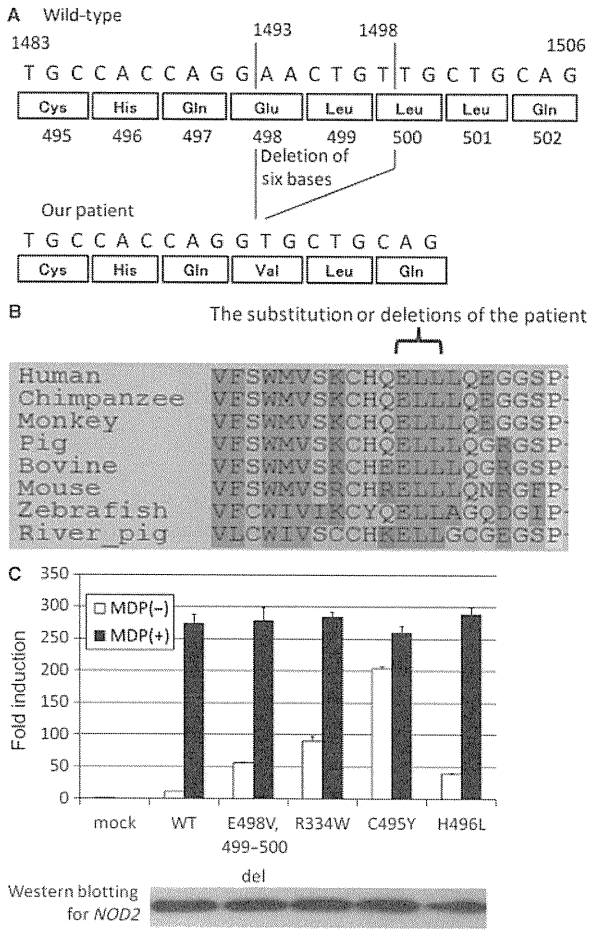

usefulness of the NF-κB reporter assay with mutant *NOD2* for observing its role in EOS/BS, although the MAP kinase activation pathway and other possible pathways need to be evaluated to more completely understand the pathogenesis of the *NOD2* mutation in EOS/BS.

We have identified the first deletion mutation in the *NOD2* gene responsible for EOS/BS, and the mutant showed constitutive activation of NF-κB, which is one of the key features that lead to the pathogenesis of EOS/BS.

Rheumatology key message

- A six-base deletion in *NOD2* gene causes EOS.

Acknowledgement

This work was carried out at Department of Pediatrics, Kyoto University Graduate School of Medicine, Kyoto, Japan.

Funding: This work was supported by grants from the Japanese Ministry of Education, Culture, Sports, Science and Technology and grants from the Japanese Ministry of Health, Labor and Welfare.

Disclosure statement: The authors have declared no conflicts of interest.

Hidemasa Sakai[1], Shusaku Ito[2], Ryuta Nishikomori[1], Yuuki Takaoka[1], Tomoki Kawai[1], Megumu Saito[1], Ikuo Okafuji[3], Takahiro Yasumi[1], Toshio Heike[1] and Tatsutoshi Nakahata[1]

[1]*Department of Pediatrics, Kyoto University Graduate School of Medicine, Kyoto,* [2]*Department of Dermatology, Hitachi General Hospital, Hitachi and* [3]*Department of Pediatrics, Kobe City Medical Center General Hospital, Kobe, Japan*
Accepted 27 August 2009
Correspondence to: Ryuta Nishikomori, Department of Pediatrics, Kyoto University Graduate School of Medicine, 54 Kawahara-cho, Shogoin, Sakyo-ku, Kyoto 606-8507, Japan. E-mail: rnishiko@kuhp.kyoto-u.ac.jp

References

1 Rosé CD, Wouters CH, Meiorin S *et al*. Pediatric granulomatous arthritis: an international registry. Arthritis Rheum 2006;54:3337–44.

2 Aróstegui JI, Arnal C, Merino R *et al*. *NOD2* gene-associated pediatric granulomatous arthritis: clinical diversity, novel and recurrent mutations, and evidence of clinical improvement with interleukin-1 blockade in a Spanish cohort. Arthritis Rheum 2007;56:3805–13.

3 Okafuji I, Nishikomori R, Kanazawa N *et al*. Role of the *NOD2* genotype in the clinical phenotype of Blau syndrome and Early-onset sarcoidosis. Arthritis Rheum 2009;60:242–50.

4 Kanazawa N, Okafuji I, Kambe N *et al*. Early-onset sarcoidosis and *CARD15* mutations with constitutive nuclear factor κB activation: common genetic etiology with Blau syndrome. Blood 2005;105:1195–97.

5 Rosé CD, Doyle TM, McIlvain-Simpson G *et al*. Blau syndrome mutation of *CARD15/NOD2* in sporadic early onset granulomatous arthritis. J Rheumatol 2005;32:373–5.

6 Chamaillard M, Philpott D, Girardin SE *et al*. Gene-environment interaction modulated by allelic heterogeneity in inflammatory diseases. Proc Natl Acad Sci USA 2003;100:3455–60.

7 Becker ML, Rosé CD. Blau syndrome and related genetic disorders causing childhood arthritis. Curr Rheumatol Rep 2005;7:427–33.

8 Kambe N, Nishikomori R, Kanazawa N. The cytosolic pattern-recognition receptor NOD2 and inflammatory granulomatous disorders. J Dermatol Sci 2005;39:71–80.

9 Hsu YM, Zhang Y, You Y *et al*. The adaptor protein CARD9 is required for innate immune responses to intracellular pathogens. Nat Immunol 2007;8:198–205.

Rheumatology 2010;49:196–197
doi:10.1093/rheumatology/kep330
Advance Access publication 25 October 2009

Comment on: Hepatotoxicity rates do not differ in patients with rheumatoid arthritis and psoriasis treated with methotrexate

Sir, We read with interest the recent article by Amital *et al*. [1] that compared hepatotoxicity rates in PsA and RA patients treated with MTX based on the evaluation of standard liver function tests. The authors conclude that the incidence of hepatotoxicity does not differ between the two disease groups after adjusting for the cumulative dose of MTX.

Several studies in MTX-treated psoriasis patients have reported that isolated abnormalities of liver enzymes (i.e. alkaline phosphatase, aspartate aminotransferase and alanine aminotransferase) were poor predictors of the severity of liver histopathology. The authors state that the combined sensitivity of aspartate aminotransferase, alanine aminotransferase and bilirubin for detecting an abnormal liver biopsy has been rated at 0.86 based on a previous study [2]. This figure implies that 14% of those with normal liver function tests will have undetected hepatic disease. Larger studies have suggested that 30–50% of the psoriasis patients on MTX have normal standard liver function test results despite histology showing fibrosis and cirrhosis [3]. The lack of correlation between liver enzymes and hepatic fibrosis and cirrhosis has been the major factor leading to the recommendation that liver biopsies be done to monitor potential hepatotoxicity. In this study, the liver function tests were performed with varying frequency which could allow abnormal liver function tests to be missed. The authors acknowledge that the rates of other hepatotoxic agents such as alcohol use and the occurrence of other hepatic comorbidities were not known. We believe that these are significant confounding variables, which make the interpretation of the results of this study difficult. The British Association of Dermatologists recommends serial monitoring

Subtypes of Familial Hemophagocytic Lymphohistiocytosis in Japan Based on Genetic and Functional Analyses of Cytotoxic T Lymphocytes

Kozo Nagai[1,2], Ken Yamamoto[3], Hiroshi Fujiwara[1,4], Jun An[1], Toshiki Ochi[1], Koichiro Suemori[1], Takahiro Yasumi[5], Hisamichi Tauchi[2], Katsuyoshi Koh[6], Maho Sato[7], Akira Morimoto[8], Toshio Heike[5], Eiichi Ishii[2]*, Masaki Yasukawa[1,4]*

1 Department of Bioregulatory Medicine, Ehime University Graduate School of Medicine, Ehime, Japan, **2** Department of Pediatrics, Ehime University Graduate School of Medicine, Ehime, Japan, **3** Department of Molecular Genetics, Medical Institute of Bioregulation, Kyushu University, Fukuoka, Japan, **4** Proteo-Medicine Research Center, Ehime University, Ehime, Japan, **5** Department of Pediatrics, Graduate School of Medicine, Kyoto University, Kyoto, Japan, **6** Department of Pediatrics, Graduate School of Medicine, University of Tokyo, Tokyo, Japan, **7** Department of Pediatrics, Osaka Medical Center and Research Institute for Maternal and Child Health, Osaka, Japan, **8** Department of Pediatrics, School of Medicine, Jichi Medical University, Tochigi, Japan

Abstract

Background: Familial hemophagocytic lymphohistiocytosis (FHL) is a rare disease of infancy or early childhood. To clarify the incidence and subtypes of FHL in Japan, we performed genetic and functional analyses of cytotoxic T lymphocytes (CTLs) in Japanese patients with FHL.

Design and Methods: Among the Japanese children with hemophagocytic lymphohistiocytosis (HLH) registered at our laboratory, those with more than one of the following findings were eligible for study entry under a diagnosis of FHL: positive for known genetic mutations, a family history of HLH, and impaired CTL-mediated cytotoxicity. Mutations of the newly identified causative gene for FHL5, *STXBP2*, and the cytotoxicity and degranulation activity of CTLs in FHL patients, were analyzed.

Results: Among 31 FHL patients who satisfied the above criteria, *PRF1* mutation was detected in 17 (FHL2) and *UNC13D* mutation was in 10 (FHL3). In 2 other patients, 3 novel mutations of *STXBP2* gene were confirmed (FHL5). Finally, the remaining 2 were classified as having FHL with unknown genetic mutations. In all FHL patients, CTL-mediated cytotoxicity was low or deficient, and degranulation activity was also low or absent except FHL2 patients. In 2 patients with unknown genetic mutations, the cytotoxicity and degranulation activity of CTLs appeared to be deficient in one patient and moderately impaired in the other.

Conclusions: FHL can be diagnosed and classified on the basis of CTL-mediated cytotoxicity, degranulation activity, and genetic analysis. Based on the data obtained from functional analysis of CTLs, other unknown gene(s) responsible for FHL remain to be identified.

Citation: Nagai K, Yamamoto K, Fujiwara H, An J, Ochi T, et al. (2010) Subtypes of Familial Hemophagocytic Lymphohistiocytosis in Japan Based on Genetic and Functional Analyses of Cytotoxic T Lymphocytes. PLoS ONE 5(11): e14173. doi:10.1371/journal.pone.0014173

Editor: Frederic Rieux-Laucat, INSERM U768, Pavillon Kirmisson, France

Received April 10, 2010; **Accepted** November 10, 2010; **Published** November 30, 2010

Funding: This work was supported by a Grant-in-Aid for Scientific Research, a Grant-in-Aid for Cancer Research from the Ministry of Health and Labor, and grants from the Ministry of Education, Culture, Sports, Science and Technology, Japan. The funders had no role in study design, data collection and analysis, decision to publish, or preparation of the manuscript.

Competing Interests: The authors have declared that no competing interests exist.

* E-mail: yasukawa@m.ehime-u.ac.jp (MY); ishiei@m.ehime-u.ac.jp (EI)

Introduction

Hemophagocytic lymphohistiocytosis (HLH) is characterized by fever and hepatosplenomegaly associated with pancytopenia [1–3]. Histologically, infiltration of lymphocytes and histiocytes with hemophagocytic activity is evident in the reticuloendothelial system, bone marrow, and central nervous system [4]. HLH can be classified as either primary or secondary [5]. Primary HLH, also known as familial hemophagocytic lymphohistiocytosis (FHL), is inherited as an autosomal recessive disorder that usually arises during infancy.

The pathogenesis of FHL has been considered to involve dysfunction of cytotoxic T lymphocyte (CTL) activity, leading to excessive production of inflammatory cytokines and macrophage activation [6]. The genetic mutations responsible for FHL have been identified by various methods. Linkage analysis has indicated two possible loci: FHL1 (MIM 603552) in 9q21.3-22, and FHL2 (MIM 603553) in 10q21-22 [7,8]. In 1999, a mutation in the *perforin* gene (*PRF1*) was identified as the cause of FHL2 [9–12]. Further genetic mutations of the *Munc13-4* gene (*UNC13D*) mapped to 17q25 (the cause of FHL3, MIM 608898) and the *syntaxin11* gene (*STX11*) mapped to 6q24 (the cause of FHL4, MIM 603552) were subsequently identified [13–15]. These mutations affect proteins involved in the transport and membrane fusion, or exocytosis, of perforin contained in cytoplasmic

granules. Recently, mutations of the *Munc18-2* gene (*STXBP2*), located in 19q, were detected as a cause of FHL5 [16,17]. Munc18-2 regulates intracellular trafficking and controls the soluble N-ethylmaleimide-sensitive fusion factor attachment protein receptor (SNARE) complex.

The molecular mechanisms underlying vesicular membrane trafficking and regulation of exocytosis have been clarified in recent years. The final step of vesicle transport is mediated by a bridge between a vesicle and its target membrane through formation of a ternary complex between a vesicle-SNARE (v-SNARE), such as a VAMP, and a target membrane-SNARE (t-SNARE), such as a syntaxin11 or a member of SNAP23/25/29 [18]. The SNARE complex is composed of three molecules: VAMP, syntaxin and SNAP23/25/29. Syntaxin11, in association with SNAP23, localizes to the endosome and trans-Golgi network [19]; however, the precise biological functions of the SNARE system are still poorly understood. Recent evidence suggests that members of the SNARE family mediate fusion of cytotoxic granules with the surface of CTLs. Syntaxin11, SNAP23 and VAMP7 are prime candidates for functioning as SNAREs in this fusion event [20].

It has been considered that clarification of the molecular abnormalities in FHL might shed light on the mechanisms of CTL-mediated cytotoxicity. Accordingly, we have been studying the functional abnormalities of CTLs in Japanese patients with FHL [21]. Our previous studies have shown that the FHL2 and FHL3 subtypes account for 20–25% of all FHL cases, respectively, whereas no FHL4 subtype exists; therefore, 45–50% of FHL cases in Japan harbor still unknown genetic mutations [21,22]. However, secondary HLH could be involved in patients with unknown genetic mutations, because both FHL and secondary HLH share similar clinical and laboratory characteristics. Therefore, in the present study aimed at clarifying the incidence and subtypes of FHL in Japanese children by genetic and functional analyses of CTLs, only patients positive for known genetic mutations, a positive family history of HLH, or impaired natural killer (NK)/CTL-mediated cytotoxicity were diagnosed definitively as having FHL.

Materials and Methods

Patients

A total of 87 Japanese children aged <15 years diagnosed as having HLH based on the diagnostic criteria of the Histiocyte Society [23] were registered at our laboratory between January 1994 and December 2009. Among them, 40 were excluded from analysis because they were diagnosed as having secondary HLH, or their parents did not provide permission for use of clinical samples. None of the patients had Chediak-Higashi syndrome, Griscelli syndrome, or Hermansky-Pudlak syndrome type 2, based on clinical and laboratory findings, including albinism or the presence of gigantic granules in lymphocytes or granulocytes. A final total of 31 patients, who met the diagnostic criteria for FHL, and for whom documented informed consent had been obtained in accordance with the Declaration of Helsinki, were entered into the study.

Genetic analysis of the *STXBP2* gene

For the detection of *STXBP2* mutations, genomic DNA was isolated from a T-cell line established from each patient. Genomic DNA (5 ng) was subjected to PCR using the primers listed in Table S1. These primer sets were designed to amplify 19 exons including the 5′-untranslated region and the coding regions with the exon-intron boundaries of *STXBP2*. The PCR products were treated with ExoSAP-IT (GE Healthcare Bio-Sciences, Little Chalfont, England) by incubation at 37°C for 15 minutes to inactivate the free primers and dNTPs, and then subjected to sequencing reactions using forward or reverse primers and BigDye® Terminator v3.1 (Applied Biosystems, Foster City, CA). The DNA fragments were purified using Magnesil (Promega, Madison, WI), and sequencing was carried out with an ABI 3730 Genetic Analyzer (Applied Biosystems). Sample sequences were aligned to reference sequences obtained from the UCSC Genome Bioinformatics website (http://genome.ucsc.edu/index.html) using the ClustalW program in order to identify nucleotide changes. Mutations were numbered according to GenBank Reference Sequence NM_001127396.1; additionally, the A of the ATG initiator codon was defined as nucleotide +1. To identify splicing variants generated by c.88-1g>a mutation of *STXBP2*, total RNA was extracted from each patient's T-cell line and reverse transcriptase PCR (RT-PCR) was performed using the forward primer on exon 1 (5′-TTGGGACACACCCGGAAG-3′) and the reverse primer on exon 5 (5′-AAGAAGATATGGGCCGCTTT-3′). The PCR products were directly sequenced using the forward primer, as described above.

Western blot analysis of MUNC18-2 protein

Expression of Munc18-2 protein encoded by *STXBP2* in T-cell lines established from FHL patients and a healthy individual was analyzed by Western blotting. CTLs were harvested after 5 days of stimulation with allogeneic LCL cells. Cell lysates were then prepared by extraction with 1% NP-40, and the extracts (10 μg per lane) were analyzed by Western blotting with anti-Munc18-2 rabbit polyclonal antibody (LifeSpan BioSciences, Seattle, WA). Horseradish peroxidase-labeled anti-rabbit IgG polyclonal antibody was used as the secondary antibody with detection by enhanced chemiluminescence (Amersham Biosciences, Buckinghamshire, UK).

Establishment of alloantigen-specific CTL lines

Alloantigen-specific $CD8^+$ CTL lines were generated as described previously [24,25]. Briefly, peripheral blood mononuclear cells (PBMCs) were obtained from FHL patients and unrelated healthy individuals. These cells were co-cultured with a mitomycin C (MMC)-treated B-lymphoblastoid cell line (B-LCL) established from an HLA-mismatched individual (KI-LCL). Using cell-isolation immunomagnetic beads (MACS beads) (Miltenyi Biotec, Auburn, CA), $CD8^+$ T lymphocytes were isolated from PBMCs that had been stimulated with KI-LCL cells for 6 days. $CD8^+$ T lymphocytes, cultured in RPMI 1640 medium supplemented with 10% human serum and 10 IU/ml interleukin-2 (Roche, Mannheim, Germany), were stimulated with MMC-treated KI-LCL cells 3 times at 1-week intervals; subsequently, these lymphocytes were used as $CD8^+$ alloantigen-specific CTL lines. The alloantigen specificity of the CTL lines was determined by assay of interferon-γ (IFN-γ) production in response to stimulation with KI-LCL cells, as described previously [24,25]. Briefly, 1×10^5 T lymphocytes were co-cultured with or without 1×10^5 MMC-treated B-LCL cells in 0.2 ml of RPMI 1640 medium supplemented with 10% fetal calf serum (FCS) in a flat-bottomed 96-well plate. In some experiments, an anti-HLA class I monoclonal antibody (w6/32; American Type Culture Collection, Manassas, VA) was added to wells at an optimal concentration. After 24 hours, the supernatant was collected from each well and assayed for production of IFN-γ using an enzyme-linked immunosorbent assay (ELISA; ENDOGEN, Woburn, MA).

Analysis of CTL-mediated cytotoxicity

The cytotoxic activity of CTLs was measured by a standard ^{51}Cr-release assay, as described previously [21]. Briefly, alloantigen-specific CTLs were incubated with ^{51}Cr-labeled allogeneic

KI-LCL cells or TA-LCL cells for 5 hours at an effector:target cell ratio (E/T) of 2.5:1, 5:1, and 10:1. Target cells were also added to wells containing medium alone and to wells containing 0.2% Triton X-100 to determine the spontaneous and maximal levels of ^{51}Cr release, respectively. After 5 hours, 0.1 ml of supernatant was collected from each well. The percentage of specific ^{51}Cr release was calculated as (cpm experimental release - cpm spontaneous release)/(cpm maximal release - cpm spontaneous release) ×100, where cpm indicates counts per minute.

Degranulation analysis by flow cytometry

Degranulation activity was analyzed by flow cytometry using anti-CD107a antibody (BioLegend, San Diego, CA) as described previously [16,17]. Briefly, 1×10^5 alloantigen-specific CTLs were co-cultured with or without 1×10^5 KI-LCL cells in 0.2 ml of RPMI 1640 medium supplemented with 10% FCS, and then FITC-conjugated anti-CD107a antibody was added to each well. After 3 hours, incubated cells were collected and analyzed by flow cytometry using PE-conjugated anti-CD8 antibody (BD Biosciences, Franklin Lakes, NJ). For analysis of degranulation, the relative log fluorescence of live cells was measured using a FACS flow cytometer (BD Biosciences).

The immunofluorescence intensities of CTLs cultured with and without alloantigen stimulation were measured, and the mean fluorescence index (MFI) was calculated as (mean value for stimulated sample – mean value for non-stimulated sample)/mean value for non-stimulated sample.

Results

Genetic subtypes of FHL patients

Among the 31 patients with FHL, 17 appeared to have *PRF1* mutation and lacked expression of perforin protein as measured by flow cytometry and Western blotting, whereas 10 patients appeared to have *UNC13D* mutation and lacked Munc13-4 protein expression as measured by Western blotting. No *STX11*

Table 1. Genetic mutations of *PRF1*, *UNC13D*, *STX11*, and *STXBP2* identified in 31 patients.

UPN	Age/Sex	*PRF1*	*UNC13D*	*STX11*	*STXBP2*
1	3 mo/F	1090.91delCT/1090.91delCT	-	-	-
2	2 mo/F	1090.91delCT/207delC	-	-	-
3	1 mo/F	1090.91delCT/207delC	-	-	-
4	11 y/F	949G>A (M)/1A>G (N)	-	-	-
5	1 mo/F	1083delG/1491T>A (N)	-	-	-
6	4 mo/F	1289insG/1289insG	-	-	-
7	1 mo/F	1349C>T (M)/1349C>T	-	-	-
8	2 mo/F	1090.91delCT/1246C>T (N)	-	-	-
9	12 y/F	1090.91delCT/1228C>T (M)	-	-	-
10	7 y/F	1349C>T (M)/1349C>T	-	-	-
11	2 mo/M	207delC/1122G>A (M)	-	-	-
12	1 mo/M	1090.91delCT/NT	-	-	-
13	4 mo/F	757G>A (M), 253G>A (M)/853-855delAAG	-	-	-
14	1 mo/F	160C>T (M), 272C>T (M)/853-855delAAG	-	-	-
15	3 mo/F	853-855delAAG/1491T>A (N)	-	-	-
16	5 mo/M	1090-1091delCT/1168C>T (N)	-	-	-
17	1 y/M	1090-1091delCT/1349C>T (M)	-	-	-
18	1 mo/M	-	640C>T (M)/-	-	-
19	6 mo/F	-	1596+1g>c (S)/1596+1g>c (S)	-	-
20	4 mo/F	-	766C>T (M)/1545-2a>g (S)	-	-
21	2 mo/M	-	640C>T (M)/1596+1g>c (S)	-	-
22	5 mo/M	-	1596+1g>c (S)/1723insA	-	-
23	5 mo/M	-	1596+1g>c (S)/754-1g>c (S)	-	-
24	6 mo/M	-	754-1g>c (S)/754-1g>c (S)	-	-
25	11 mo/M	-	1596+1g>c (S)/322-1g>a (S)	-	-
26	1 mo/M	-	754-1g>c (S)/2163G>A (N)	-	-
27	2 mo/F	-	322-1g>a (S)/754-1g>c (S)	-	-
28	2 mo/M	-	-	-	292-294delGCG/88-1g>a
29	2 mo/M	-	-	-	1243-1246delAGTG/1243-1246delAGTG
30	0 day/M	-	-	-	-
31	0 day/F	-	-	-	-

UPN, unique patient number; M, male; F, female; -, not detected, NT, not tested.
In parenthesis, M means missense mutation, N means nonsense mutation, and S means splicing abnormality.
doi:10.1371/journal.pone.0014173.t001

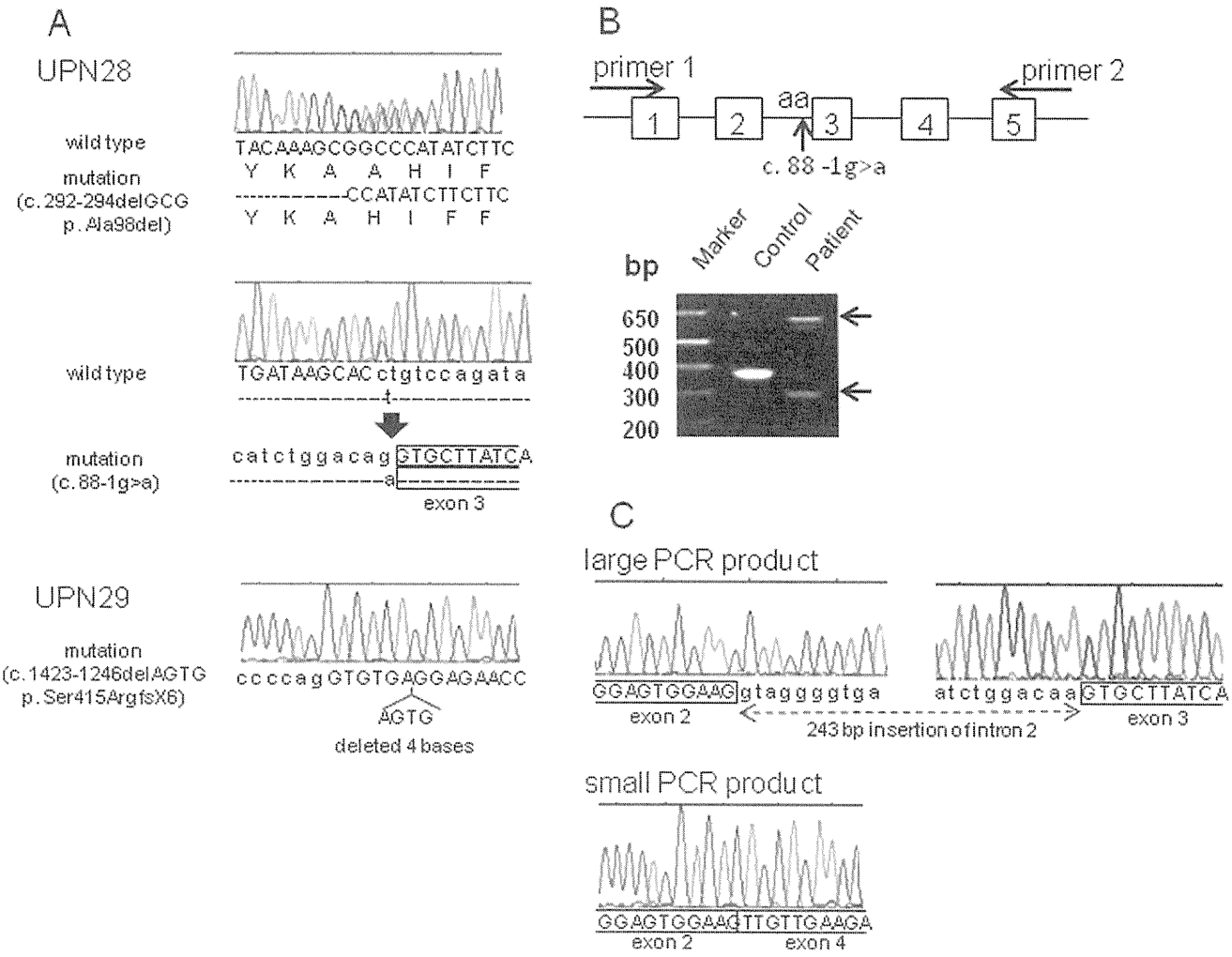

Figure 1. Identification of *STXBP2* mutations. (A) Sequencing analysis of 4 patients with non-FHL2/3/4 and detection of 3 novel mutations in 2 of them: a compound heterozygous mutation of 292_294delGCG resulting in Ala98del at exon 5 (upper panel) and 88-1g>a in intron 2 (lower panel) in one patient (UPN28), and a homozygous mutation of 1243-1246AGTG resulting in Ser415ArgfsX6 at exon 15 in the other (UPN29). (B) Expression of *STXBP2* cDNA in UPN28 with 88-1g>a mutation. Schematic representation of positions of the primers for RT-PCR and 88-1g>a mutation is shown in the upper panel, and for RT-PCR products from 88-1G>A mutation of *STXBP2* in the lower panel. The expected 350-bp product of *STXBP2* exons 1–5 was detected in a healthy control individual, whereas extra larger- and smaller-sized products were detected in UPN28 (arrow). (C) Sequence analysis revealed that the 88-1g>a mutation retained the entire intron 2 (243 bp) in the cDNA. This insertion is predicted to cause addition of 81 amino acids to the N-terminal region of the large Sec1 domain of the Munc18-2 protein (upper panel). Sequence analysis of the smaller fragment revealed that the mutation caused skipping of exon 3 (82 bp), resulting in a frame shift and translational arrest after an additional 20 amino acids (lower panel).
doi:10.1371/journal.pone.0014173.g001

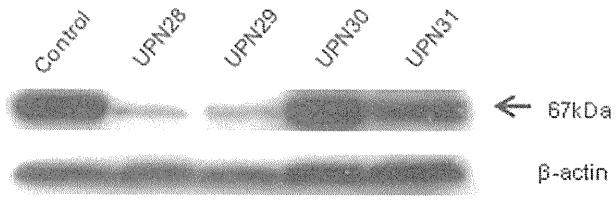

Figure 2. Western blot analysis of Munc18-2 protein expression. Expression of Munc18-2 protein in each $CD8^+$ T-cell line that had been stimulated with allogeneic B-LCL cells was analyzed by Western blotting using anti-Munc18-2 antibody. Munc18-2 protein was abundantly detected at 67 kDa in CTL lines established from healthy control individuals and 2 non-FHL2/3/4/5 patients (UPN30, and UPN31).
doi:10.1371/journal.pone.0014173.g002

mutations were detected in any of the patients (Table 1). Most of the data have been reported elsewhere [11,12,14,21,22,26]. For the remaining 4 patients (UPN28-31), *STXBP2* mutation and CTL function were further analyzed.

STXBP2 analysis and Munc18-2 expression in 4 patients with non-FHL2/3/4

Genetic analysis of *STXBP2* was performed in 4 patients with non-FHL2/3/4 (UPN28-31). As shown in Fig. 1A, a compound heterozygous *STXBP2* mutation with 292_294delGCG and 88-1g>a was detected in UPN28, and a homozygous mutation with 1243_1246delAGTG appeared to be present in UPN29. These 3 mutations of *STXBP2* are all novel. RT-PCR analysis showed that 2 aberrant cDNAs were produced in UPN28 (Fig. 1B). Sequence analysis revealed that the large fragment 88-1g>a mutation caused insertion of the entire intron 2 (243 bp) into the cDNA,

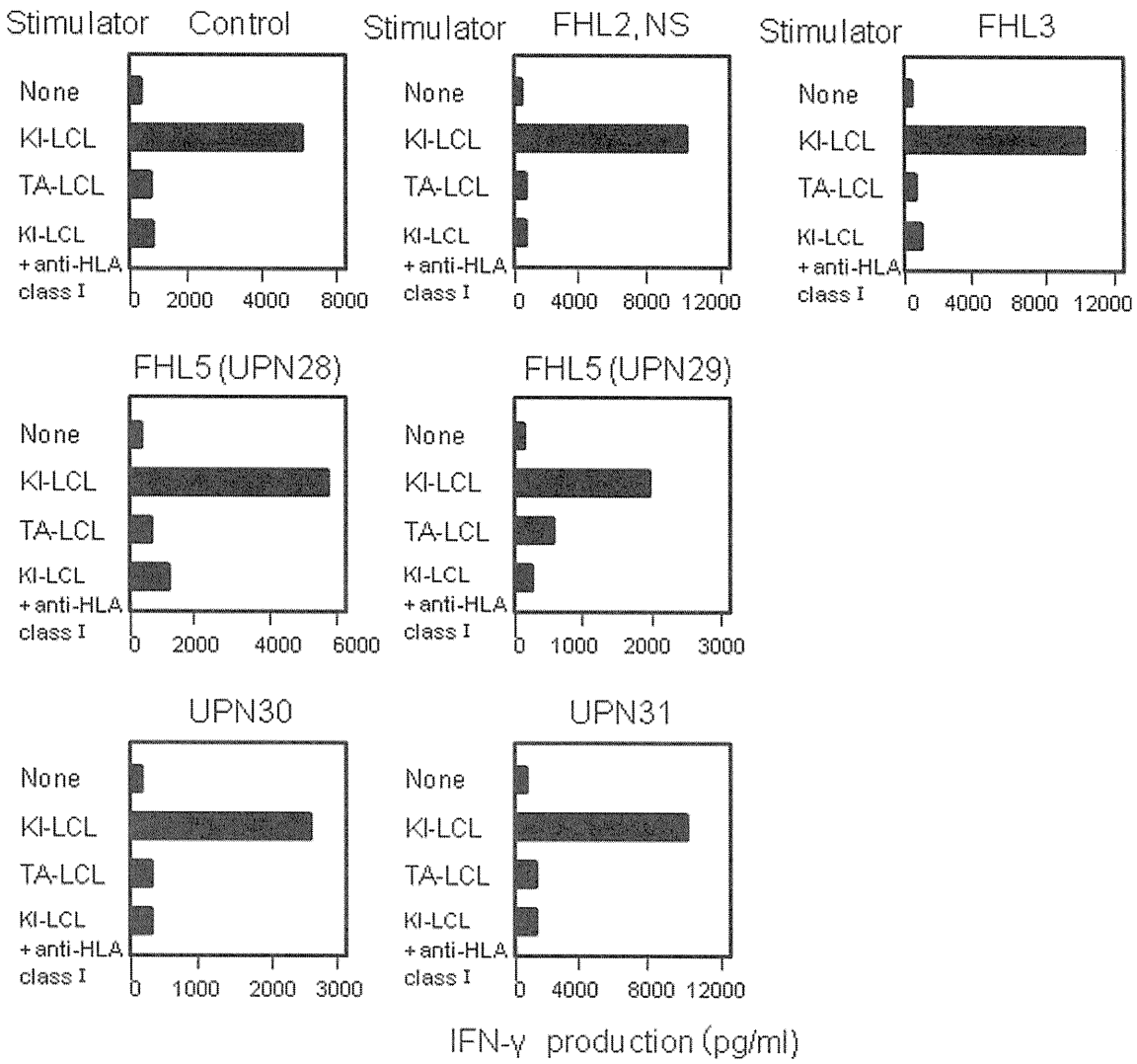

Figure 3. IFN-γ production by alloantigen-specific CD8$^+$ T cell lines. CD8$^+$ T-cell lines were generated from the PBMCs of the patients with FHL and healthy individuals as controls by stimulation with allogeneic B-LCL (KI-LCL) cells. Responder cells were co-cultured with or without KI-LCL or TA-LCL, which shared no HLA antigens with KI-LCL, in the presence or absence of anti-HLA class I monoclonal antibody for 24 hours. IFN-γ production was measured by ELISA. All FHL patients showed normal production of IFN-γ. The HLA type of KI-LCL is HLA-A01/30, B13/17, Cw6/-, DRB1*0701/*0701, and that of TA-LCL is HLA-A24/26, B62/-, Cw4/w9, DRB1*0405/*0901. NS indicates *PRF1* nonsense mutation.
doi:10.1371/journal.pone.0014173.g003

while in the small fragment the mutation caused skipping of exon 3 (82 bp), resulting in a frame shift and translational arrest after an additional 20 amino acids (Fig. 1C).

We analyzed the expression of Munc18-2 protein in CTLs of these 4 patients using Western blotting. As shown in Fig. 2, the Munc18-2 protein band at approximately 67 kDa was scarcely detectable in 2 FHL patients with *STXBP2* mutation (UPN28, UPN29). On the basis of these data, these 2 were diagnosed as having FHL5. On the other hand, Munc18-2 protein expression was clearly detected in CTL lines established from the remaining 2 patients (UPN30, UPN31); therefore, these patients were considered to have FHL with unknown genetic mutations.

Functional analysis of CTL lines established from FHL patients

Alloantigen-specific CD8$^+$ CTL lines were generated from healthy individuals, and from patients with FHL2 (UPN8), FHL3 (UPN23), and non-FHL2/3/4 (UPN28-31). The antigen specificities of the T-cell lines were examined by measuring their IFN-γ production in response to stimulation with allogeneic LCL cells. As shown in Fig. 3, all alloantigen-specific CD8$^+$ T-cell lines generated by stimulation with allogeneic KI-LCL produced large amounts of IFN-γ in response to stimulation with KI-LCL cells, but not with TA-LCL cells, which share no HLA antigens with KI-LCL. These results indicated that T lymphocytes of FHL patients can respond normally to antigen stimulation and produce inflammatory cytokines. Their IFN-γ production was significantly abrogated by anti-HLA class I antibody, indicating that the responses of these T-cell lines were alloantigen-specific and HLA class I-restricted.

Cytotoxic activity mediated by CD8$^+$ alloantigen-specific T-cell lines generated from healthy individuals (n = 24) and FHL patients are measured, and the representative data are shown in Fig. 4. Antigen-specific cytotoxicity mediated by CTLs from FHL2 patients with *PRF1* nonsense mutation was entirely deficient, whereas that of CTLs from FHL3 patients with *UNC13D* splicing abnormality was low but still detectable, as we have reported